LANGMUIR AND LANGMUIR BLODGETT STUDIES OF CADMIUM SELENIDE (CdSe) QUANTUM DOTS

A THESIS SUBMITTED TO
THE GRADUATE SCHOOL OF NATURAL AND APPLIED SCIENCES
OF
MIDDLE EAST TECHNICAL UNIVERSITY

BY

ZUHAL SELVİ VANLI

IN PARTIAL FULFILLMENT OF THE REQUIREMENTS
FOR
THE DEGREE OF MASTER OF SCIENCE
IN
CHEMISTRY

OCTOBER 2017

Approval of the thesis;

LANGMUIR AND LANGMUIR BLODGETT STUDIES OF CADMIUM SELENIDE (CdSe) QUANTUM DOTS

submitted by **ZUHAL SELVİ VANLI** in a partial fulfillment of the requirements for the degree of **Master of Science in Chemistry Department, Middle East Technical University** by,

Prof. Dr. Gülbin Dural Ünver _____
Dean, Graduate School of **Natural and Applied Sciences**

Prof. Dr. Cihangir Tanyeli _____
Head of Department, **Department of Chemistry**

Prof. Dr. Mürvet Volkan _____
Supervisor, **Department of Chemistry**

Assoc. Prof. Dr. Murat Kaya _____
Co-supervisor, **Department of Chemical Engineering and Applied Chemistry, Atılım University**

Examining Committee Members:

Prof. Dr. Ali Çırpan _____
Chemistry Dept., METU

Prof. Dr. Mürvet Volkan _____
Chemistry Dept., METU

Assoc. Prof. Dr. Murat Kaya _____
Chemical Engineering and Applied Chemistry Dept., Atılım University

Assoc. Prof. Dr. Gülay Ertaş _____
Chemistry Dept., METU

Assist. Prof. Dr. Çiğdem Ay _____
Chemistry Dept., Dumlupınar University

. **Date:** 04.10.2017

I hereby declare that all information in this document has been obtained and presented in accordance with academic rules and ethical conduct. I also declare that, as required by these rules and conduct, I have fully cited and referenced all material and results that are not original to this work.

Name, Last name: Zuhal Selvi VANLI

Signature:

ABSTRACT

LANGMUIR AND LANGMUIR BLODGETT STUDIES OF CADMIUM SELENIDE (CdSe) QUANTUM DOTS

VANLI, Zuhal Selvi

M. S., Department of Chemistry

Supervisor: Prof. Dr. Mürvet Volkan

Co-supervisor: Assoc. Dr. Murat Kaya

October 2017, 92 pages

Various methods can be used to prepare layered thin films with the sensitivity of molecular level. Langmuir Blodgett method, draws attraction since its discovery both in thin film production and in transferring the films produced onto a solid surface. Langmuir films have the application areas of biosensors, coating studies, electronic molecular and optoelectronic devices and semi-permeable barriers.

In this work, firstly the alignment of silver nanoparticles on air water interphase was planned. Therefore, to provide optimum conditions for LB film of silver nanoparticles we tried to obtain stable cetyltrimethylammonium bromide (CTAB) films on deionized water subphase. However, at low concentration of CTAB (0.07 mg/mL) we could not get stable monolayers.

To increase the stability of monolayer of CTAB, a new technique namely “gluing technique” was used and its effect on the stability of CTAB monolayers were investigated by using Poly(4-styrenesulfonate) (PSS) as gluing reagent. As a result of

both surface pressure versus mean molecular area (π – MMA) isotherms and hysteresis experiments it was concluded that more stable monolayers of CTAB were obtained at low concentration with gluing technique.

However, in the continuation part of the study; hoping that the fluorescence emission of the nanoparticles that were arranged on the surface can be seen by using hand-hold UV light, we decided to prepare LB thin films of Cadmium Selenide (CdSe) quantum dots instead of silver nanoparticles. Their synthesis and characterization were done by thermal decomposition method and fluorescence spectrometry respectively. The emission intensity of the QDs, at the excitation wavelength of 400 nm, was observed at 558 nm. The morphological characterization of quantum dots was done with Transmission Electron Microscopy (TEM).

The monolayer formation of CdSe quantum dots and their mixture with stearic acid (SA) were achieved on water air sub-phase. During these studies, parameters corresponding compression rate and volume of CdSe quantum dots that spread onto sub-phase were optimized. Addition of SA as a spacer was improved spreading property of QDs and consequently facilitated the stable monolayer formation.

Langmuir monolayer of CdSe quantum dots deposited on to the glass substrates and first characterization of these layers were done with Confocal Microscopy. In accordance of the information acquired with confocal microscopy, the selection of thin films of quantum dots that would be characterized by TEM was selected. TEM patterns have clearly shown that the homogeneous and closely arranged CdSe quantum dots films were obtained on the entire surface of the substrate.

Keywords: Langmuir, Langmuir Blodgett, thin films, quantum dots, CdSe quantum dots

ÖZ

KADMİYUM SELENÜR (CdSe) KUANTUM NOKTALARIN LANGMUIR VE LANGMUIR BLODGETT ÇALIŞMALARI

VANLI, Zuhal Selvi

Yüksek Lisans, Kimya Bölümü

Tez Yöneticisi: Prof. Dr. Mürvet VOLKAN

Ortak Tez Yöneticisi: Doç. Dr. Murat KAYA

Ekim 2017, 92 sayfa

Moleküler düzey hassasiyetinde katmanlı ince filmlerin hazırlanmasında çeşitli yöntemler kullanılmaktadır. Langmuir Blodgett metodu keşfinden bu yana hem film oluşturma hem de oluşturulan filmlerin katı yüzey üzerine aktarılması açısından ilgi çekmektedir. Bu metot ile oluşturulan filmlerin biyosensör, yüzey kaplama elektronik moleküler ve optik cihazlar ve seçici geçirgen bariyerlerin oluşturulması gibi uygulama alanları vardır.

Bu çalışmada, öncelikli olarak gümüş nanoparçacıkların dizilmesi öngörülmüştür. Dolayısıyla gümüş nanoparçacıkların LB filmi için optimum koşulları sağlamak amacı ile saf su alt fazında kararlı setiltrimetilamonyum bromür (CTAB) filmleri elde edilmeye çalışılmıştır. Bununla birlikte, CTAB' ın düşük derişimde (0.07 mg / ml) kararlı tek tabakaları elde edilememiştir.

CTAB LB tek katmanlarının kararlılığını arttırmak için, yapıştırıcı malzeme olarak suda çözünür bir polimerler olan Poli (4-stirensülfonat) (PSS) kullanımının etkisi

araştırılmıştır. Alt faz olarak PSS’ nin farklı derişimdeki sulu çözeltileri hazırlanarak, PSS derişiminim ve sıkıştırma hızının CTAB' ın tekli tabaka oluşturması üzerine etkisine bakılmış ve katmanın kararlılığı histerez (tekrarlı sıkıştırma açma) deneyleri ile sınanmıştır. Yapıştırma tekniği ile CTAB 'ın daha kararlı tek tabakalarının hazırlanabileceği sonucuna varılmıştır.

Bununla birlikte, çalışmanın devam eden bölümünde; UV ışığı kullanarak yüzeyde dizilecek kuantum noktalarının emisyonunu görmeyi ve bu yolla kaplama işleminin başarısını TEM görüntüsü almadan sağlamayı planlayarak gümüş nanoparçacıkları yerine Kadmiyum Selenür (CdSe) kuantum noktalarının kullanımı ile LB ince filmlerini hazırlamaya karar verdik.

CdSe kuantum noktalarının sentezi termal bozunma yöntemi ile yapılmıştır. Kuantum noktaların karakterizasyonu flüoresans spekrometrisi ile yapılmıştır. 400 nm'lik uyarım dalga boyundaki emisyon yoğunluğu 558 nm'de gözlenmiştir. Kuantum noktaların morfolojik karakterizasyonu ise Geçirimli Elektron Mikroskobu (TEM) ile yapılmıştır.

CdSe kuantum noktalarının LB tek tabaka flimlerinin oluşturulması ile ilgili çalılşmalar yapılmıştır. Bu kapsamda, farklı sıkıştırma hızları ve yüzey üzerine dağıtılan CdSe kuantum noktaların hacimleri optimize edilmiştir. CdSe kuantum noktalarının Langmuir tek tabaka davranışları, bir aralayıcı (spacer) olarak stearik asit (SA) mevcudiyetinde de incelendi. SA eklenmesi kuantum noktaların alt faz yüzeyinde yayılma özelliğini geliştirmekte ve kararlı tek tabaka oluşumunu kolaylaştırmaktadır.

CdSe kuantum noktalarının Langmuir tekli katmanları katı yüzey üzerine aktarılmış ve bu katmanların karakterizasyonu Konfokal Mikroskobu ile yapılmıştır. Buradan edilen bilgi yardımıyla CdSe kuantum noktaların ince filmi, Geçrimli Elektron Mikroskobu ile karakterize edilmiş ve quantum noktaların homojen olarak, aralarında hiç boşluk kalmayacak şekilde dizilmiş ve katı yüzeyin tüm yüzeyinin kaplamış oldukları gözlemlenmiştir.

Anahtar Kelimeler: Langmuir, Langmuir Blodgett, ince filmler, kuantum noktalar, CdSe kuantum nokta.

to my precious family…

ACKNOWLEDGMENTS

Firstly, I would like to thank my supervisor Prof. Dr. Mürvet VOLKAN for her endless guidance, support and mostly encouragement. I have learned everything that I know during three years from her.

I want to thank my co-advisor, Assoc. Prof. Dr. Murat KAYA, for his unique knowledge and guidance.

I wish to express my sincere gratitude to Prof. Dr. Atilla CİHANER, Assoc. Prof. Dr. Belgin İşgör, Assoc. Prof. Dr. Seha TİRKEŞ in ATILIM University for their valuable support and understandings.

I want to thank Assoc. Prof. Dr. Çağdaş SON for his valuable support during the characterization studies.

I want to thank Asst. Prof. Dr. Çiğdem AY for her valuable support and understanding when I felt hopeless.

I would like to thank Yeliz AKPINAR for her valuable knowledge, support, encouragement and understanding and patience. She was always with me anytime when I needed. It was really an excellent experience for me working with her and learning how to think in chemistry.

I would like to give my special thanks to Pakizan TASMAN and Merve AKPINAR for their support and their help whenever I need.

I want to express my appreciation Begüm AVCI, Canan HÖÇÜK, Merve Nur GÜVEN and Sezin ATICI for their friendship and funny activities.

I also want to thank Elif DEMİR and Tuğrul AKPOLAT for their friendship, coffee times and their support whenever I need about my computer.

I cannot explain my feelings about Şeyda, Özge G., Sezil, Müge, Sacide Özlem, Oya, İpek, Yasemin, Özge A. and Gülşah with just few words. They were with me during my whole university life and after graduation. Anytime I need, they were ready for me. They will always be my friends.

I also want to thank Cavidan Güner and Erkan Güner for their support. With the presence of them, my family is larger now.

I would like to thank my mother Muazzez VANLI, my father Ahmet VANLI and my sisters Şeyda VANLI, Ayşegül VANLI and Ceren VANLI for everything. My family is the strongest family that I know. They never leave me alone and supported me always for my every decision. I know that they are always on the next side of me regardless the kilometres. I appreciate their existence.

Finally, I would like to thank Emre for his love, trust, support, patience and understandings. He always made me happy and laugh whenever I felt sad and hopeless. I am the luckiest person in the world since I could find him. I am very glad you are here next to me.

TABLE OF CONTENTS

LIST OF FIGURES

FIGURES

LIST OF TABLES

TABLES

LIST OF ABBREVATIONS

^{o}C	degrees Celsius
Å	angstrom
µL	microliter
π	surface pressure
A	area
CdSe	Cadmium Selenide
CTAB	Cetyltrimethyl ammoniumbromide
CTMS	Chlorotrimethylsilane
DI	Deionized
L	Layer
LB	Langmuir-Blodgett
mg	milligram
mg/mL	miligram per mililiter
mL	milliliter
mm	milimeter
mM	milimolar
MMA	mean molecular area
mm/min	millimeter per minute
mmol	millimole
mN/m	milinewton per meter
nm	nanometer
PSS	Polystyrenesulfonate
rpm	round per minute
SA	Stearic acid
TEM	Transmission Electron Microscopy
TOPO	Tiroctylphosphine oxide
TR	Transfer ratio
QD	Quantum Dot

CHAPTER 1

INTRODUCTION

1.1. Methods for Preparation of Thin Films

By virtue of knowing the variety of organic compounds and their molecular properties, there is a good deal of methods to prepare organic thin films [1]. To clarify, these methods can be listed as, self-assembled monolayers, Langmuir Blodgett method, layer by layer method, solution evaporation, thermal evaporation and electrochemical deposition [2, 3].

To start with self-assembled monolayers, generally obtained as a result of the interaction of the material that has strong affinity to the substrate surface that is patterned on it [4]. They are divided into two groups mainly chemisorbed and physisorbed monolayers [3]. The former one is the result of the chemical interaction between substrate and adsorbate. The second one can be defined as the binding of the adsorbate to substrate that interaction is rather low. When chemisorption and physisorption is compared due to the strong interactions such as hydrogen bonding, ion pairing etc. chemisorption assemblies are more stable [4].

Langmuir Blodgett method provides organization of the molecules on a liquid surface and deposition of the this organized molecule monolayer with molecular thickness of the studied one [5]. After the formation, transfer of the monolayer could be done by dipping the solid substrate vertically called as Langmuir- Blodgett method and horizontally that is named as Langmuir- Schaefer method [6]. The system is attractive to studies due to the providing the molecular thickness thin films for many applications and control the structure of the films at molecular level in terms of orientation and placement of the molecules throughout the monolayer and

multilayer assembly [5].

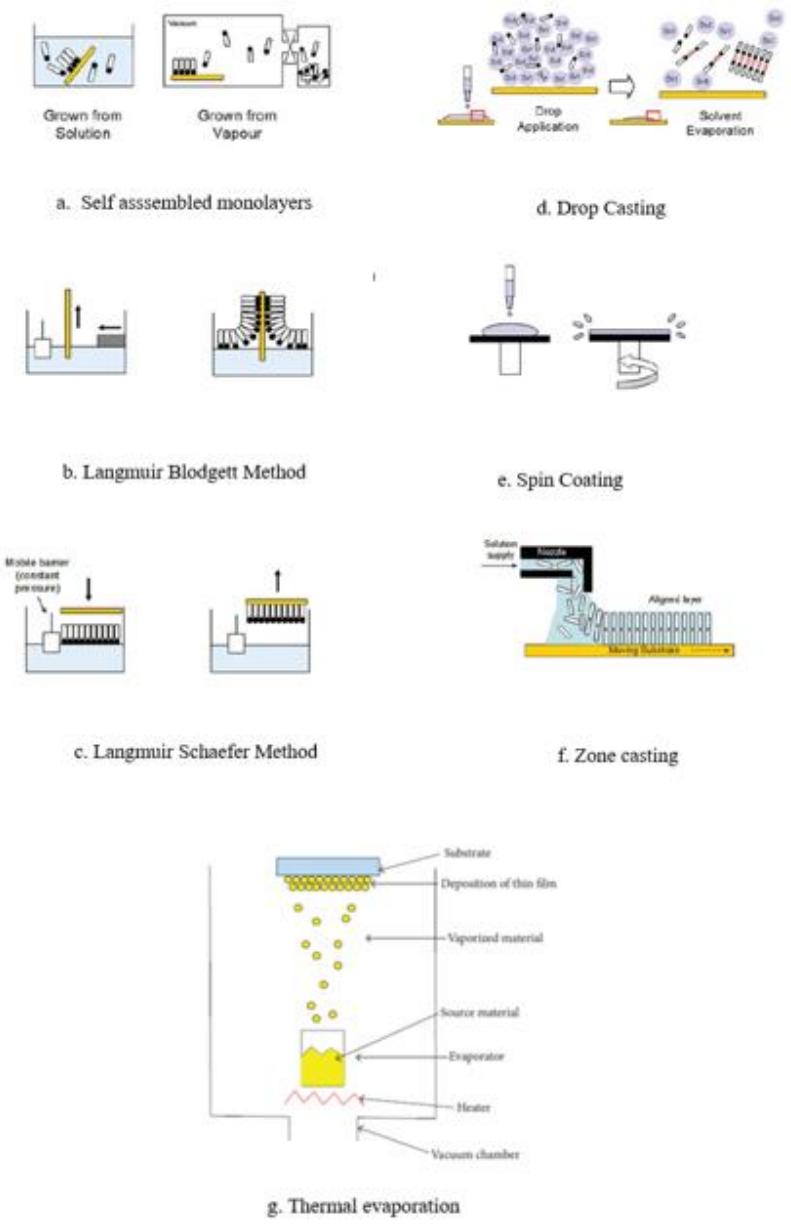

Figure 1 The simple schemes some of the summarized method [1,7].

The layer-by-layer (LbL) assembly is introduced in 1991 and until now it is the one of the main method to prepare thin films with nanostructures. The process includes the adsorption of a charged species on an opposite charged of surface of substrate

firstly. Secondly, depending on the aim of the thickness of the film, with controlling surface charge layers are deposited on to substrate subsequently. Beside the electrostatic interaction, on the basis of covalent bonding, hydrogen bonding, hydrophobic interactions the LbL approach can be applicable for broad range of materials on various substrates [8].

Moreover, to obtain thin films solvent evaporation, thermal evaporation, electrochemical deposition methods may be used. Solvent evaporation is the process of depositing nanostructures with controlling the solvent evaporation. Drop casting, spin coating and zone casting methods are the examples for solvent evaporation method. In drop casting process, a small volume of solution is dropped onto substrate and it is left to dry under air or atmosphere of solvent to provide slower evaporation. Spin coating includes the evaporation of the solvent and pushing of the excess solution as a result of the placing the substrate onto a high-speed spinning wheel. During the rotation due to the surface tension residue of the material is observed on the substrate. Although, this method is generally applicable for polymers, it may be improved for nanostructures. Zone casting method consists of a nozzle that provides solution continuously onto a moving substrate. Over the solution supplying solvent evaporation occurs through the surface of the meniscus that is formed between the substrate and special flat of the nozzle. This method renders the oriented anisotropic layers of soluble molecules onto a not oriented substrate. Thermal evaporation method is the oldest method to prepare thin films. The method depends on the vacuum deposition of a material onto a substrate with sublimation due to heating by current. The nature and purity of the material, cleanliness and roughness of substrate, evaporation rate and the temperature are important parameters for this method. The molecules that are stable under sublimation temperatures and high vacuum equipment are also necessity of this method. Lastly, the electrochemical deposition is the electrochemical oxidation of neutral molecules with the presence of the proper counter ion electrolyte that is concluded with deposition of the conducting charge transfer salts on an electrode which is used as substrate [3]. Some of the mentioned methods are summarized as schematically in Figure 1.

Within these methods while zone casting method provides highly oriented films covering large areas, drop casting and spin coating can be applicable for relatively small areas. Thermal evaporation method provides the control of the thickness of the film from one to several monolayers with the help of complementary characterization techniques when compared with zone casting method [3]. When SAM, LB and LbL methods are compared; while SAM approach provides uniform single layer formation and LbL method gives multi layered films, both monolayer and multi-layered films are obtained with LB method. The other advantage of LB method is applicability of this method with both hydrophilic and hydrophobic materials. However, SAM and LbL approaches applicable with water soluble materials [2]. Beside these advantages of the LB system, LB method needs a longer time periods for formation of monolayer and multilayers and expensive instrumentation [9].

1.2. Langmuir and Langmuir Blodgett Method

1.2.1. History of Langmuir Films

The beginning of the surface chemistry related to Langmuir Blodgett method start with Benjamin Franklin in the 18th century with spreading a 2 mL oil on a 2000 m^2 lake. After spreading he observed the 2 ml oil had coated one fourth over the lake and he proposed that there was an oil layer with 1 nm thickness over the lake considering the volume of the oil and area of the lake [10]. After Franklin, about in 1882 Agnes Pockels manipulate the oil films on the water while she was working in the kitchen [11]. Moreover, she designed the first model of the Langmuir trough [12]. In 1899, Lord Rayleigh helped Pockels and proposed the thickness of the layer was one conception of the molecular conformation and indicate the identical orientations of the molecules due to their hydrophilic and hydrophobic characteristics. Langmuir also suggested that this obtained monolayers could be deposited onto a solid support and his assistant Katherine Blodgett studied on the deposition of the monolayer onto a solid support vertically in 1934-1935. A few years later, Langmuir and Vincent Schaefer developed a method, called as Langmuir Schaefer that provides the deposition of the monolayer onto a solid support horizontally [12].

1.2.2. Theory of Langmuir and Langmuir Blodgett Films

To reduce free energy a number of organic molecules try to organize themselves at the interface of gaseous- liquid phase or liquid- liquid phase. Consequentially, the surface film of the molecule is formed that has one molecule thick and called as monomolecular layer or monolayer [13].

The Langmuir monolayer film formation starts with the spreading the solution of the material, surface active agents, on the subphase. The monolayer film is formed with compression on the subphase after the evaporation of the subphase insoluble solvent of the solution. During this formation surface active reagents molecules goes into the gas phase to solid phase which is observed during the experimental procedure from surface pressure to area isotherm. The formation of monolayer on air liquid interface is summarized in Figure 2.

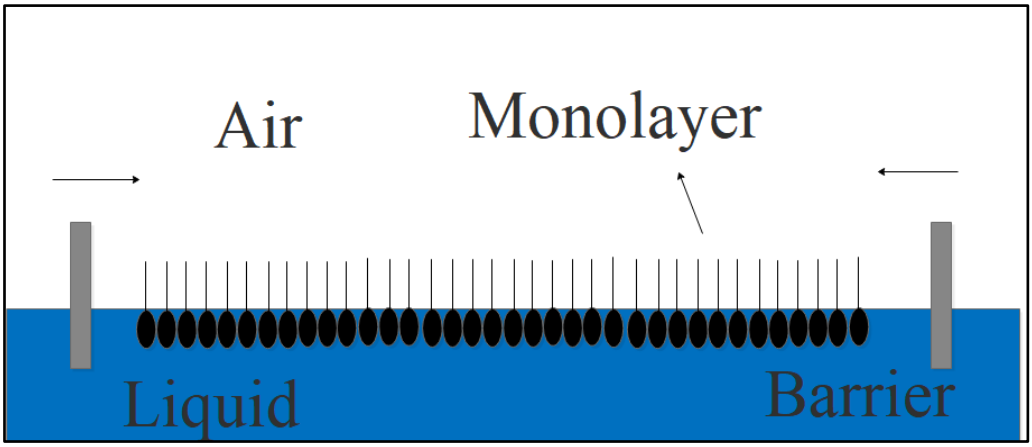

Figure 2 Simple Scheme of Langmuir Blodgett Monolayer

1.2.2.1. Subphase

The trough of the LB system filled with subphase depending on the desired experiment the system is adjusted for the experiment. While mercury, and also glycerol can be used as a subphase, deionized water is the most commonly used one [14].

1.2.2.2. Surface Active Reagents

According to the chemistry studies; materials can be classified as water soluble or not. While the water-soluble materials called as hydrophilic the latter ones named as hydrophobic and the materials that have both hydrophilic and hydrophobic character is defined as amphiphilic or surface-active reagents. Amphiphilic molecules are the main monolayer material for the LB system. The hydrophilic group stays in water favourably and the hydrophobic group pushes it away from the water surface preventing the molecule from dissolving in the water at the interface of air and water [14].

Beside surface active reagents, LB technique is applicable for aromatic compounds, polymers, dyes, biological compounds and nanoparticle [15, 17].

1.2.2.3. Surface Pressure - Area Isotherm

Surface tension is the most significant concept throughout the interface studies with fluid bulk phases. The environmental difference between the molecule and the molecule in the bulk results in the extra free energy on the surface of the liquid and this excess energy defined as the surface tension [18].

As in the LB system, if there is a monolayer on the surface instead of surface tension the surface pressure term is used. The determination can be examined by Wilhelmy plate, and the surface pressure that is equal to reduction of the surface tension of the pure liquid with the presence of monolayer can be defined as;

$$\Pi = \gamma_0 - \gamma$$

In the equation; γ_0 and γ indicate the surface tension of the pure liquid and surface tension of the monolayer covered the surface respectively. As a subphase as mentioned earlier water is more preferably, with its high surface tension that is 73 $mN.m^{-1}$ at 20℃ [13] .

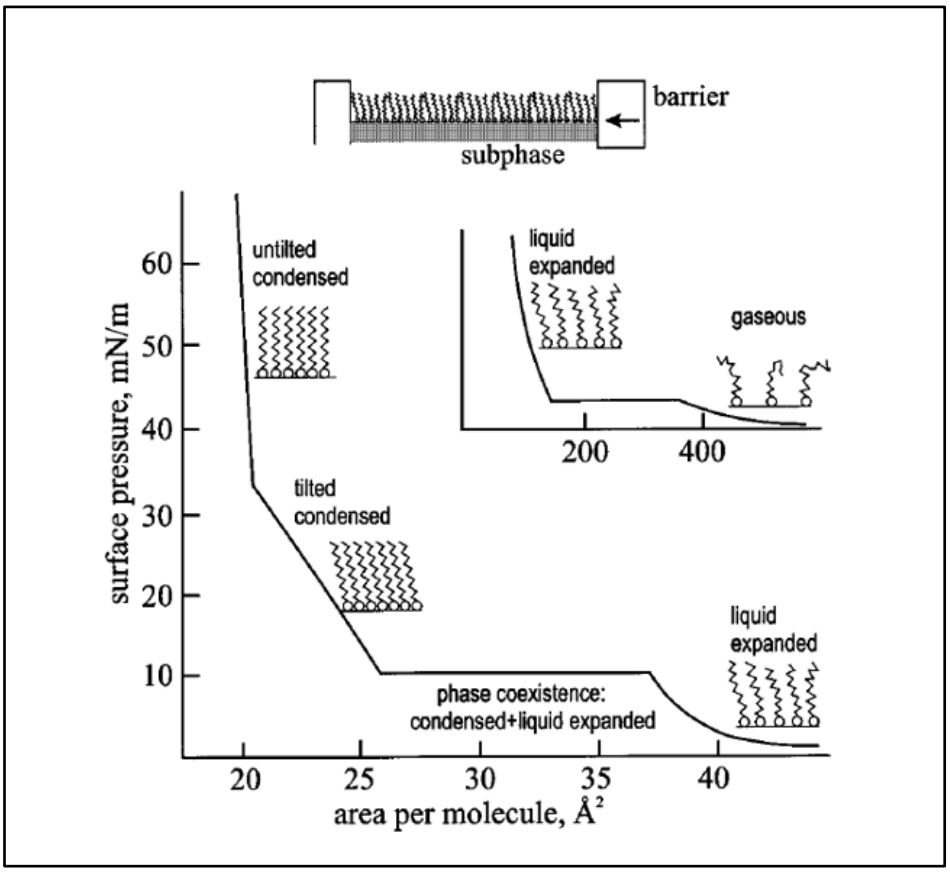

Figure 3 Example for area per molecule versus surface pressure isotherm for a fatty acid [19]

Area depending on the experiment may be trough area, total area or mean molecular area. Mean molecular area is calculated for each material that is studied by entering some parameters to interface program. The mean molecular area (a) is calculated by dividing the total film area to number of molecules with the help of the formula;

$$a = AM / CN_AV$$

where A is the total film area, M is molar mass of the material, C is concentration of the solution and V is volume of the spread solution [13].

Surface pressure area isotherm gives information throughout the formation of the monolayer on the surface of the subphase during the compression. The surface pressure area isotherm shows an alteration depending on some parameters; nature of

the material, spreading conditions, temperature and compression speed. Generally, the isotherm has four transition regions, gaseous (G) phase, liquid expanded (LE) phase, liquid condensed (LC) phase and solid (S) phase respectively. In Figure 3 the isotherm for a fatty acid is summarized as an example for a isotherm. With the compression that is increasing the surface pressure; the monolayer proceeds from two-dimensional G phase to LE expanded phase and continued compression the phase goes into LC from LE. In this phase, molecules are translationally and chains of the molecules conformationally disordered. Between these transition phases (G to LE and LE to LC) first order transition takes place indicating plateau (pseudo) region. With the continuous compression, the phase of the monolayer goes into S phase where maximum surface pressure is reached. This maximum surface pressure is called as the collapse point. After collapse point the monolayer become deformed and molecules are overlapped. The all phase transitions may not be present for all amphiphilic molecules relying on the experimental conditions [19, 20] .

1.2.3. Deposition of Langmuir Monolayers

The transfer of obtained monolayers onto a solid support from the air water interface is feasible via Langmuir Blodgett technique or Langmuir Schaefer technique. The first one is the vertical deposition that is transfer of the monolayer takes place through the vertical displacement of a solid substrate. In the second method, deposition is done horizontally; transfer of the monolayer is done on the solid substrate that moves horizontally above the monolayer [14]. Langmuir Blodgett and Langmuir Schaefer methods are shown in Figure 4 schematically. The surface pressure of the monolayer controlled firstly so that the monolayer is stable and in the condensed form. This stability conditions depend on the type of the materials. Generally, there is a limitation for surface pressure should be between 20 – 40 mN/m that related with the collapse point and rigidity of the monolayer. Beside this, there is also possibility to start deposition any state of monolayer [13].

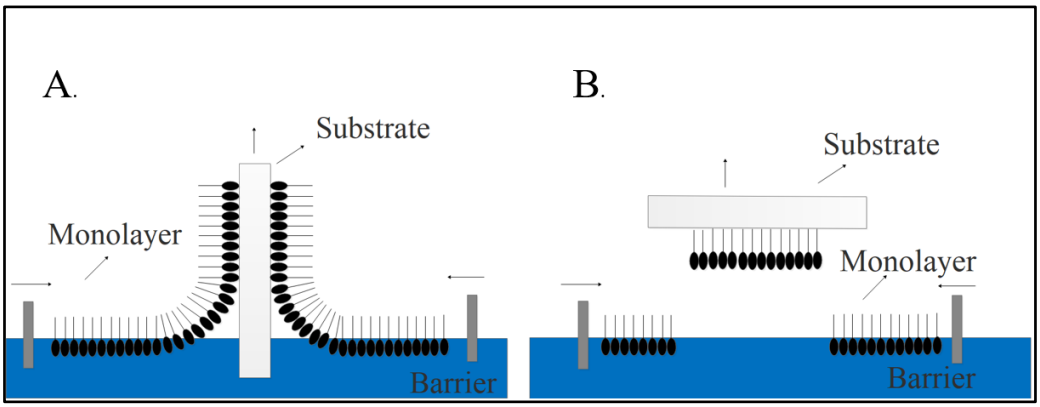

Figure 4 Simple schematic illustration of A. Langmuir Blodgett Method and B. Langmuir Schaefer Method

For Langmuir Blodgett system three types of deposition may be observed which are named as Y type, X type and Z type. This Y, X and Z type callings do not define the obtained layers, they just give information about the deposition type. The deposition of the monolayer with subsequent movement of the substrate in and out of the surface and continued with this trend provides Y type dipping. When the deposition of the monolayer occurs on the trend of downstrokes and upstrokes these type of dippings refer to Z type and X type respectively (interfacial science). In Figure 5 after these deposition types the illustrations are summarizing the placement of amphiphilic molecule. With the prominence of optimum surface pressure for the deposition depending on the desired experiment for X, Y and Z type dipping surface modification of the substrate must have done before dipping studies.

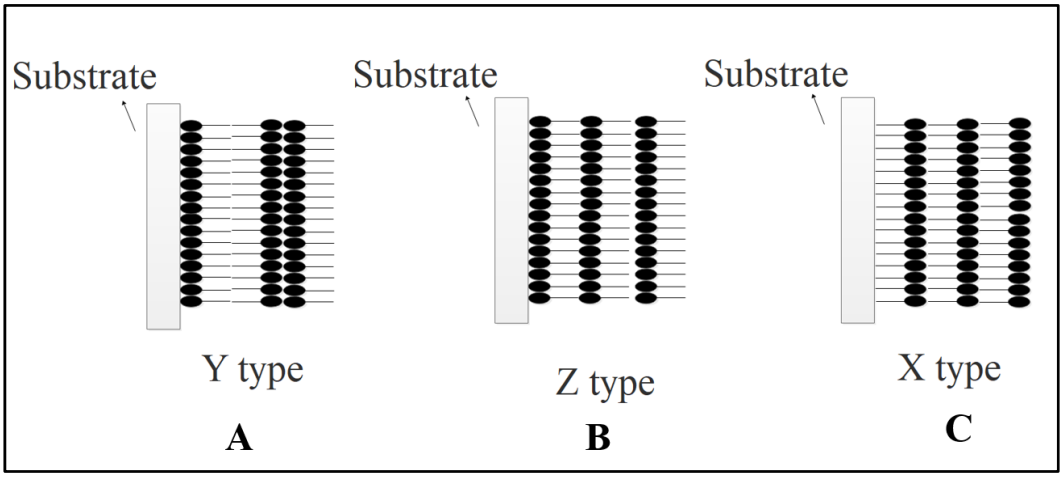

Figure 5 Types of Langmuir Blodgett multilayers A. Y type, B. Z type, C. X type

1.2.4. Applications of Langmuir and Langmuir Blodgett Films

The technique of Langmuir is a unique and an elegant method for molecular level organization and orientation of the materials. The properties of the materials depend on their organizations and at this point the Langmuir film formation has a significant role for applications of these materials.

The method is just not applicable for surfactants and lipids it is applicable for various materials that form monolayer on the water surface [6].

Firstly, polymers are used as a LB material due to their stronger mechanical and thermal stabilities compared to other materials. Conducting polymers are also used in the LB films due to their biocompatibility. They are combined with organic materials for biosensor applications [6, 21-22].

Moreover, the complex formation with aqueous polyelectrolytes provides the stabilization of charged Langmuir monolayers. Example of this stabilization is done in the studies of Regen and named as the gluing of the layers. In the study of Regen calix [6]- arene layers are glued with poly(4-styrenesulfonate) (PSS) by adding to subphase to form bilayer. These glued layers have the application of the gas permeation selectivity. Moreover, gluing provides robustness, reduce the formation defects of monolayer and improves the cohesiveness of the films [23, 24].

In recent years, two dimensional nanomaterials and their assembly have interest due to mechanical and optical properties for scientific studies and industrial applications. For this aim the thin film of magnetic nanoparticles is also studied for their promising applications such as sensors, magnetic storage media, nano-optoelectronics, labelling and sorting of cells, separation of biomedical applications due to their magnetism and low toxicity. In the study of Kezheng Chen and his co-workers has the example of patterned $CoFe_2O_4$, Fe_3O_4 and Fe_2O_3 magnetic LB films. Moreover, in the study of Young Soo Kang Fe_3O_4 magnetic nanoparticles are stabilized with stearic acid to form a monolayer to be useful for the fabrication of ultra-high density magnetic storage media [25, 26].

Langmuir Blodgett method may result in new concepts with nanostructured materials (nanoparticles, carbon nanotubes). This combination provides new materials with new properties that is not accessible with other methods. As a result of this, many hybrid and patternable materials construction attemptions are studied with Langmuir Blodgett technique in terms of electronic and molecular electronic devices, polymeric membranes, organic light emitting diodes (OLEDs) and plastic solar cells [27].

Beside many nanoparticles LB technique is also applicable for hydrophobic colloidal quantum dots that are increasingly becoming popular. The combination of quantum dot with LB method has the application area of biosensors, light harvesting devices, photodetectors due to size dependent properties of quantum dots. High photostability of quantum dots enable to improve application of quantum dots in biological research group such as fluorescence imaging tools. In the study of Goto and his co-workers cell extracts from cancerous and non-tumorigenic cells spread onto surface with the incorporation of CdSe quantum dots. After the deposition of formed monolayer, morphology characterization of the film was done with AFM and Confocal Microscopy. Further results indicated that the membrane model of cells and CdSe QDs formed with the Langmuir Blodgett method provides device application for cancer diagnosis [28, 29].

1.3. Quantum Dots

Ostwald named his famous book as ‘’The World of Neglected Dimensions’’ related to colloid chemistry in 1915. When considered the dependence of the physical and chemical properties of colloids on their size and shape, the name of the book corresponds the idea [30] .

The word nanostructure is used for the definition for a solid that indicates significant diversities in terms of optical and electrical properties due to their different size that is smaller than 100 nm. To this respect, the gap between bulk and molecular levels of nanostructured materials provides new perspectives in terms of applications in biology, electronics and optoelectronics [31].

To state briefly, when the charge carriers of the semiconductor material are limited into a specific area that has the dimensions equivalent or less than de Broglie wavelength of the carriers by potential barriers, the diameter of nanocrystal is less than the Bohr radius of excitons in the bulk phase of the material and results in the dramatic quantization effects. The confined charge carriers with the effect of potential barriers in three spatial dimensions, the coverage of space is titled as quantum dot. Based on their confinement dimensions nomenclature changes. The two-dimensional confinement fabricates quantum wires or rods and one-dimensional confinement creates quantum films. The synthesis of quantum dots can be done via two methods; epitaxial vapor deposition that can include molecular beam epitaxy and metallic organic chemical vapor deposition or chemical synthesis that can be either colloidal chemistry or electrochemistry. Occasionally nanocrystal term is used to refer quantum dots although the term includes shapes other than spherical; such as nanowires, nanotubes, nanoribbons, nanorings, nanorods and nanotetrapods [32].

To summarize and with some addition to first definition, inorganic semiconductor nanostructured materials that composed of atoms of periodic groups of II-VI, III-V or IV-VI elements defined as quantum dots. For the most part, they contain close to 200 – 10000 atoms with a diameter between 2- 8 nm spherical shape [33].

1.3.1. Properties of Quantum Dots

Semiconductor quantum dots are tiny crystalline particles that indicate size dependent optical and electrical properties. By bridging the gap between small molecules and large crystals, they show distinct electronic transitions similar to isolated atoms and molecules with providing the development of the worthwhile features of the quantum dots. The minimum energy that is needed for the excitation of an electron from ground state valence energy band to the vacant conduction energy band is defined as band gap energy and this energy is characteristic for the characterization of bulk semiconductors. Due to the absorption of a photon that has energy greater than band gap energy; an orbital hole is formed in the valence band with the excitation of an electron. At this point, positively charged hole and negatively charged electron may be activated with electric field to yield a current considering situation of the lowest energy state of the electron-hole pair that is the electrostatically bound between the electron and hole pair, known as the exciton. The exciton is annihilated with the relaxation of the excited electron to the valence band that can come with the emission of a photon is the process named as radiative recombination. Exciton that depends on the material from 1 nm to more than 100 nm variable Bohr exciton diameter has a finite size in crystal that is identified. When a semiconductor quantum dot has a smaller size than the exciton size, the charge carriers become limited spatially that provides increasing of the energy of the quantum dot. As a result, the transition between the regulation of properties of bulk crystal and the regime of quantum confinement which is the dependence of the optical and electrical properties on the size of the quantum dot defined by exciton. Therefore, quantum dots having dimensions smaller than Bohr exciton diameter indicates size dependent fluorescence and absorption spectra with distinct electronic transitions [34].

Quantum dots are also defined as the particles that are semiconductor nanocrystals and have physical dimension smaller than the exciton Bohr radius. When a visible light photon hits a quantum dot, some of the electrons excite into higher energy states. After that with the returning of the electron to ground state, a photon with a characteristic frequency of the material is emitted [35].

Due to their synthetic routes quantum dots are categorized as colloidal and epitaxial in other words self-assembled quantum dots. While colloidal quantum dots are synthesized wet chemical approaches the latter ones synthesized through dry methods from the vapor phase. Colloidal quantum dots also known as solution-processed quantum dots and they draw attention due to their potential application as high quality photodetector [36, 37].

The synthesis of colloidal quantum dots mainly includes the three-component system comprised of precursors, organic surfactants and solvents. The precursors turn into monomers when reaction medium is heated to adequately high temperature. After reaching the super saturation level of monomers, with nucleation process the growth of quantum dots proceeds. One of the key detail throughout the synthesis is determining the optimum temperature conditions for the growth of quantum dots [36].

Semiconductor colloidal quantum dots have been studied for more than two decades in terms of both experimentally and theoretically. Lately, they draw attention as a possible material for optoelectronic applications. The solution processibility of colloidal quantum dots ensures completion with an almost variety of substrates. Comparing to the epitaxial quantum dots, colloidal quantum dots have the benefits of easy processing, low cost, large area coverage and physical flexibility [36].

Quantum dots have unique electrical and optical properties due to the quantum confinement effects. This quantum confinement results in the many advantages compared to organic dyes, and fluorescent proteins. The quantum confinement affects particularly the properties related to fluorophore behaviour including the photostability, the width of emission and excitation spectrum and decay lifetime and this situation increases the applicability possibility. Other than the photochemical applications of quantum dots, they also attract attention due to their feasible biological applications. Conventional dyes are also used for biological applications, but they suffer from the necessity of excitation with a specific wavelength. They have broad emission spectra which means there is a possibility of overlapping of spectra of many dyes and as a result limitation of the number of fluorescent probe

that may be used for different biological molecules is observed. Compared to the conventional dyes, quantum dots have controllable narrow emission spectra with modifiable of core size, composition and surface coating. In the size range of 2 - 6 nm of semiconductor quantum dots have respectable interest also for biological applications since they have similar dimension with biological macromolecules. Quantum dots are suited into the multiplexed imaging that is the combination of multiple colours and intensives to protein, encode genes and small molecules. Beside this photostability of quantum dots provide monitoring the interactions of multiple labelled biological molecules in cells for a long time [35] .

The incomparable size dependent properties of quantum dots make them active research area progressively with the application of optoelectronic and biomedical technologies. After the first synthesis of quantum dots, thin films of quantum dots have specific characteristics in the application range of optoelectronic devices for instance; solar cells, light emitting devices, photodiodes, photoconductors. Moreover, solutions of quantum dots used in numerous techniques that are in vivo and in vitro imaging, labelling and sensing [37].

1.3.2. Properties of Cadmium Selenide (CdSe) QDs

In comparison to many emitting species semiconductor quantum dots have the advantages of possibility of altering the emission colour just by changing the size of the quantum dots and providing perfect colour purity [38].

Colloidal quantum dots have the property of excellent photostability large spin orbiting coupling and narrow emission line widths compared to other organic chromophores. Therefore, they are promising materials for use in solution processable thin film optoelectronic devices [39].

The grand improvements in colloidal chemistry provide the preparation of high quality several semiconductor quantum dots. Among these, CdSe quantum dots have the extensive research time probably due to providing the control of the size, shape and monodispersity during the synthesis methods [40].

QDs comprised of cadmium (Cd) and selenium (Se) absorb and emit visible radiation particularly, provides to observation of size dependent quantum phenomena visually. Beside this Bohr radius of CdSe quantum dots makes study on quantum confinement effect over the broad range of size available [41].

From the case of CdSe quantum dots due to their adjustable emission colour from blue to red makes them most promising emitting material [38].

In terms of synthesis over the quantum dots, CdSe QDs has the most developed system. As a result of this development nearly monodisperse size and shape of CdSe QDs makes them active in industrial development of biological labelling reagents [42].

Colloidal CdSe quantum dots are highly emissive inorganic particles that have a spherical shape with a few nanometres diameters. Depending on the size of the quantum dot they have electronic properties as a result of the quantum confinement. In future photonics applications of semiconductor quantum dots have a significant place due to their different wavelength response by varying the size of the quantum dots [43].

1.3.3. Synthesis of CdSe QDs

To synthesize high quality CdSe quantum dots different methods are demonstrated that includes safe common and low-cost compound as a solvent and precursors. These alternative methods provide the manageable manner for the size range from about to 1.5 nm to above 25 nm, shape and crystal structure throughout the synthesis of quantum dots [44].

For the synthesis, as a cadmium precursor cadmium chloride ($CdCl_2$) may be used to synthesize quantum dots by one pot approach organometallic route. However, $CdCl_2$ did not work well though it is not soluble at elevated temperatures according to the Peng and Peng's study. At this point they supposed that the stability of cadmium oxide (CdO) was lower than the stability of $CdCl_2$ relative to phosphonic acids that was the advantage for the one pot synthesis of CdSe quantum dots. According to the

studies of Peng that the synthesis was not sensitive as it was thought. CdSe quantum dots can be obtained in several solvent systems that comprise of phosphine oxides, amines and fatty acids and mixture of these chemicals at certain compositions. Throughout the several experiments; CdO was desired cadmium precursor for the synthesis of quantum dots that contain cadmium such as cadmium telluride (CdTe), CdSe and cadmium sulfide (CdS) to compare with dimethyl cadmium ($Cd(CH_3)_2$) according to the two different studies of Peng. Beside, cadmium acetate ($Cd(Ac)_2$) and fatty acids might be used as a cadmium precursor and solvent and the results of again Peng's studies indicated that as a cadmium precursor $Cd(Ac)_2$ and other types of cadmium carboxylate were versatile due to their medium since they were utilizable in the presence of phosphonic acid or fatty acid [42, 44].

As a solvent in the study of Peng and his co-workers octadecene was selected due to its low cost, relatively low melting point and high boiling point, low toxicity, low reactivity to precursors and high solvation power for many precursors at elevated temperatures to grow high quality quantum dots. Moreover, oleic acid was favoured natural surfactant ligand for stabilizing the quantum dots [44, 46].

1.3.4. Langmuir and Langmuir Blodgett Studies of CdSe Quantum Dots

The development studies indicate the significant advances of evolvement of quantum dot synthesis providing the controllable size, shape, surface chemistry and composition. The application the QDs with these unique properties requires the assembly of quantum dots. Monolayer of quantum dots have been used for the design of light emitting diodes while multi layers of assembled quantum dots are used as multicolored light emitting films, light harvesting devices, biosensors photodetectors. For the efficiency of these applications the quality and the controllability of the monolayer and multilayers is essential. To obtain this aim several approaches have been reported. One of them is layer by layer (LbL) assembly with usage of polymer linker by spin assisted LbL assembly with the requirement of hydrophilic in other words water soluble particles. On the other hand, to fabricate monolayer or multilayer of hydrophobic particles onto a substrate an effective method Langmuir

Blodgett or Langmuir Schaefer method might be used at the air water interface. Over the other methods LB and LS method provided deposition of closely packed QD layer onto a large area [47].
Organized arrays of colloidal CdSe quantum dots on the large area provided many applications inclosing hybrid organic- inorganic solar cells, light emitting devices and photonics [48].

The utilization of colloidal CdSe quantum dots needs well defined mono or multilayers of the assemblage of quantum dots. In the study of Hens and co-workers to obtain such layers Langmuir Schafer method was used and for the characterization of these layers, atomic force microscopy, transmission electron microscopy and UV-vis absorption spectroscopy was offered. In the same study at the beginning of the compression in the graph of surface pressure versus area might not be result in increment due to the decrease in the closing of the gaps and continuous compression provided the merging of the monolayer islands into a closely packed monolayer was also reported. The study also indicated that the importance of substrate hydrophobicity onto resulting layer structure. As a result, cellular networks or smooth layers with containing different stacking organization could be obtained [47].

In the study of Tanushree Bala and his co-workers Langmuir Blodgett method had been used to provide assembly of nanoparticles with providing easy control in film thickness in materials science and this makes the technique popular. This method was used for the deposition of the miscellaneous materials including quantum dots onto solid surface to obtain long range assembly. In the study for the mechanism of the formation of the monolayer of oleyl amine coated CdSe QDs was proposed on the competent capping ability of oleyl amine that makes the quantum dot hydrophobic. At the subphase when particles were exposed to the $HAuCl_4$ at an acceptable surface pressure that is the monolayer was in the most compact arrangement, the restriction of movement of CdSe QDs was suggested a mechanism for the formation of the monolayer [49].

In the study of Subhasis Das's, by using Langmuir and Langmuir Blodgett films of lipids as membrane model the specific interaction of CdSe QDs with tumorigenic

and non-tumorigenic cells for diagnosis of cancerous cells was studied. In the work CdSe QDs was merged into the Langmuir monolayers of lipids that is obtained on the at the air water interface with the extracts of tumorigenic and non-tumorigenic cells. The main idea was proposed as usage of the film that is obtained with cells and incorporation of the CdSe QDs. This manner was used to compare and analyze the effects of the selected constituents on the films and investigate the physical and chemical properties. The observation of after addition of the cells on to the air water interface the isotherm surface pressure versus to area revealed rather in liquid phase with indicating high compressibility values due to the addition of cells that contains high number of constituents such as lipid and biomacromolecules was also explained. For the same study, the microscopy confocal images for tumorigenic and non-tumorigenic cells with CdSe QDs were taken. According to the images with non-tumorigenic cells the contrast was similar to DPPC performing homogenously distributed non-agglomerated CdSe QDs over the scanned film area while with tumorigenic cells the distinction of fields due to agglomeration of QDs was reported. The results were interpreted as the indication of the result of interaction of the QDs with normal cells no alteration while the significant alterations were observed for tumorigenic cells and this difference was proposed as a model for the cancer diagnosis [29].

According to Hampton and his colleagues by incorporating microcontact printing or Langmuir-Blodgett method the gathering of the QDs could be obtained using up-down production methods. For large-scale fabrication required for photovoltaic applications was not suitable with the Langmuir-Blodgett technique since production of QD monolayer indicated a relatively low efficiency process [48] .

On the other hand; in the study of Matthew D. Goodman’s owing to unique and promising photo physical properties for use in optoelectronic devices composites of semiconductor quantum dots and electroactive conjugated polymer had been the focus of the study area. As a summary, the semiconductor P3HT-CdSe nanocomposites in the air - water interface formed by Langmuir isotherms were investigated. The size of the nanocomposites was found as expected according to the results from the Langmuir isotherms. Depending on the experimental results,

improvement of photovoltaic performance with incorporating QDs into conjugated polymer- quantum dot nanocomposites that was obtained as a thin film with Langmuir Blodgett method was reported [50] .

QDs indicates solubility in several nonpolar solvents owing to the intrinsic ligand that they are synthesized. Trioctylphosphine oxide (TOPO) that contains three alkyl chains provides the solubility of quantum dots in polar solvents such as chloroform, hexane and cyclohexane. Moreover, TOPO capped CdSe quantum dots form a stable monolayer at the air water interface owing to the phosphorous oxygen bond of TOPO that provides a large dipole moment to the quantum dots. The stability of Langmuir monolayer film was substantial while working with ligands that surrounds QDs since the stability decreases due to wettability at the air water interface and increasing nanoparticle size. TOPO ligand is weakly bounded to surface of the QD though it was stable at temperatures much greater than the other surroundings. Although TOPO may be replaced with other strongly bound surfactants for instance thiolates, the stability of the TOPO capped quantum dots observed with kinetic measurements provided most stable Langmuir film with dithiocarbamate (DTC) and 1-octadecanethiol (ODT) as an alternate due to their stability and reproducibility. However, DTC aggregates rapidly compared to the TOPO coated QDs [51] .

According to the molecular modelling and experimental calculations demonstrated that TOPO surfactants combined with the other TOPO ligands of the neighbouring quantum dots and formed a close packed Langmuir monolayer at the air water interface. In the same study Langmuir films of QDs analyzed in terms of photoluminescence property and the relation between the property with increasing number of layers was examined. TOPO capped quantum dots were deposited onto quartz slides and deposition occurred at the higher surface pressures indicated an increment in the photoluminescence intensity owing to the closer packed structure of the quantum dots. For the both hydrophilic and hydrophobic quartz slides the intensity increased linearly with the addition of each layer of quantum dots onto the substrate. In the TEM studies of Langmuir monolayers of CdSe quantum dots indicates that the quantum dots organized into a hexagonal structure of closely packed nanoparticles in each layer [51].

By using Langmuir monolayers, the surface chemistry of CdSe and CdSe(ZnS) core shell quantum dots were also tried to be characterized and various techniques were reported briefly. The different regions of the isotherms during the formation of the monolayer were observed throughout the compression process by surface pressure area isotherm. Moreover, these regions also observed as local hexagonal packing of the quantum dots with the help of HR-TEM. Furthermore, due to the manipulation of the films by using ligand exchange with TOPO and ODT was also studied and the latter one resulted in the limitation to nanoparticle area and minimal influence on the optical properties in terms of absorption and emission of the particles. Qwing to these methods, Langmuir Blodgett films permits for the analyzing of the packing structure of Langmuir monolayers throughout the various characterization methods. Besides, Langmuir technique was reported as an efficient and progressive method that provides information about the interaction at the two-dimensional level in a controlled environment, while being a convenient tool for examining single layers of QDs [51] .

1.4. Aim of Study

In this study, firstly the Langmuir Blodgett studies of silver nanoparticles was aimed. For this purpose, Langmuir monolayer of CTAB were studied. Gluing technique with PSS was used to obtain stable monolayer of CTAB since at low concentration (0.07 mg/mL) of CTAB was not obtained on deionized water subphase. The optimization studies were done and formation stable monolayer of CTAB with gluing effect of PSS were observed. However, after hoping to observe monolayer formation of quantum dots under UV light we started to study on monolayer of CdSe quantum dots. At this point this study has three aims: Firstly, to synthesize trioctylphosphine oxide (TOPO) coated 2-4 nm CdSe QDs and characterize them buy using Fluorescence Spectroscopy and Transmission Electron Microscopy. Secondly, after synthesis and characterization of the CdSe QDs to obtain thin film of QDs the monolayer formation on the water air interface will be studied. To reach this aim, spread volume of the solution and compression rate of the barriers will be optimized. Throughout this, the optimum conditions will be observed to deposit the monolayer on the solid surface. Thirdly, finding out the optimum conditions for optimum

monolayer formation for deposition types was examined. Furthermore, the deposited film was characterized on the TEM grid.

CHAPTER 2

EXPERIMENTAL

2.1. Materials

Hexane (≥ 95%), acetone (C_2H_6O, ≥ 99%) chloroform ($CHCl_3$, ≥ 99.8%), methanol (CH_3OH ≥ 97%) and ethanol (C_2H_5OH ≥ 99.8%) were purchased from Sigma-Aldrich. Cadmium oxide (CdO, powder ≥ %99.5), trioctylphosphine oxide (TOPO), oleic acid ($C_{18}H_{34}O_2$≥93%), hexadecyltrimethylammonium bromide (CTAB, 99%), poly(4-styrenesulfonate) (PSS, 30 wt % in H2O, av. MWt: 70000) were provided from Sigma-Aldrich. Octadecene ($C_{18}H_{36}$ ≥ 95%) was obtained from Fluka. Selenium (Se) was purchased from Fisher Scientific. Hydrogen peroxide (H_2O_2, 35%), ammonia (25%) and chlorotrimethylsilane (CTMS, ≥ 99%), were purchased from Merck. Deionized water, 18.2 MΩ.cm from Elga, Purelab Option-Q Water Purification System was used throughout this study.

2.2.Instrumentation

2.2.1. Fluorescence Spectroscopy

Fluorescence characterization of quantum dots was done by using HITACHI F-2500 type fluorescence spectroscopy.

2.2.2. System of Langmuir Blodgett Film Formation

Minimicro Langmuir-Blodgett (LB) film formation system comprised of a Polytetrafluoroethylene (PTFE) trough, platinum Wilhelmy plate, dipper motor and 2

barriers manufactured by KSV, Finland was used to prepare the monolayer and multilayer films.

2.2.3. Transmission Electron Microscopy

For the visualization of the both quantum dots and monolayer and multilayers on TEM grid; JEOL JEM 2100 F model transmission electron microscopy was used.

2.2.4. Contact Angle

In order to determination of surface modification Attension Theta contact angle instrument manufactured from KSV Instruments was used.

2.2.5. Hand- Held Ultraviolet Lamp

For the observation of synthesized QD solution on a glass slide under UV light, UVP UVGL 6 -Watt handheld UV lamp (254 nm and365 nm) was used.

2.2.6. Centrifuge

Nuve brand NF 200 model centrifuge was used for the preparation of the pureCdSe quantum dots.

2.2.7. Confocal Microscopy

For the images of the deposited films of the CdSe quantum dots on the glass substrate Leica branded confocal microscopy was used.

2.2.8. Vortex

During the washing step of CdSe quantum dots Heidolph branded vortex was used.

2.3. Cleaning of Langmuir Blodgett System

Cleaning is the most critical step of the experiments for preparation of high quality of the monolayer on air water subphase. For this aim before starting the experiments; calibration and cleaning steps should be followed carefully. A standard weight with a known value was measured by balance to calibrate the Langmuir Blodgett system. During the cleaning procedure firstly, trough was cleaned with chloroform to remove any sediment. Then platinum Wilhelmy plate was washed with deionized water, acetone and chloroform. At this point acetone is used as intermediate solvent between deionized water and chloroform. Finally, the barriers were cleaned with ethanol, rinsed with deionized water and dried by wiping.

2.4. Isotherm Experiments

Before starting any experiment, cleaning procedure was applied thoroughly. After opening the barriers to obtain the maximum area, trough was filled with sub-phase up to the mark line on the walls. Wilhelmy plate was also immersed into subphase partially. Both balance and barrier position were zeroed and pureness of subphase checked by the balance value. If the balance was above the 0.2-0.3 mN/m surface of the subphase was cleaned by vacuum aspirator. After all conditions checked a known volume of a highly dilute solution was spread onto the surface as small droplets with the help of a micro syringe. The software program opens a file for each experiment and parameters of the experiment such as target value for the compression, volume, concentration, subphase, compression rate of the barriers were entered as the inputs. A certain time (10 min.) was waited for the evaporation of the solvent before the formation of the layer and the system starts compression at a determined rate of the barriers after the evaporation time. With the defined compression rate of the barriers amphiphilic molecules that were disordered initially getting closer and ordered and monolayer was formed. During the formation of the monolayer; information of the phase transformation and the surface pressure where the monolayer was formed was monitored simultaneously and in compliance to entered parameters at the beginning the π -MMA isotherm that is marked as surface pressure versus mean molecular area was obtained. From this isotherm graph, instantaneous information such as the

surface pressure, mean molecular area, trough area /area and barrier position were readable.

In the obtained isotherms, for π- MMA and π-A, the ideal isotherm has all phase transitions gas, liquid and solid. At the end of the solid phase the deformation of the monolayer is observed, and this point is named as collapse point. Yet, for all surfactants or all compounds these phase transitions could not be observed. These topics were mentioned in 1.2.2.3.

2.5. Surface Modification of Glass Substrate

For the deposition of the monolayer, glass slides (13 x 13 mm having thickness 0.13-0.17 mm) were used. Depending on the desired result of the experiment, surface of glass slides was modified as hydrophilic or hydrophobic. Before hydrophilic treatment glass slides were rinsed with soapy water to remove residues and dried with nitrogen (N_2) gas. Hydrophilic treatment was applied with base piranha solution that prepared by adding hydrogen peroxide (H_2O_2, %25) to ammonia (%25) in 1:1 volume ratio. To obtain hydrophobic surfaces; glass slides were treated as hydrophilic as reported before and then they were stored in 0.2 M chlorotrimethylsilane hexane solution for 2 hours at room temperature and washing with deionized water and drying with N_2 gas procedures were applied respectively. The treatment summary in terms of surface chemistry is shown in Figure 6.

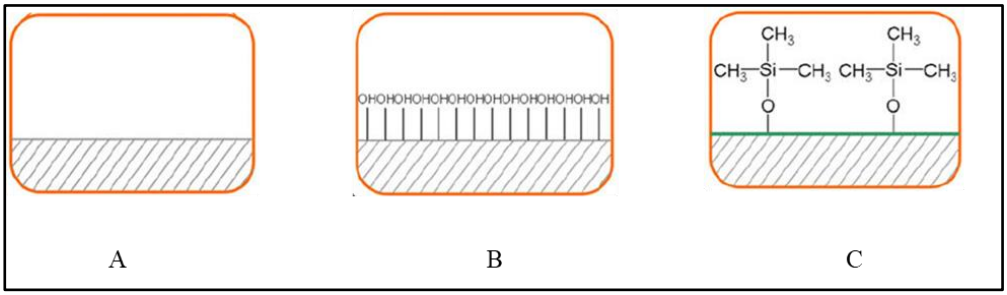

Figure 6 Scheme of surface modification of glass substrate; A: surface of glass substrate, surface of glass substrate after; B hydrophilic treatment, C hydrophobic treatment [52]

2.6. Deposition of Monolayers onto a Solid Support

As in isotherm experiments all cleaning procedure was applied as well for the deposition of monolayer experiments. Depending on the desired experiment the treated substrate was attached to the dipping arm of the instrument and the zero line where the substrate touched the surface of the subphase was settled. The substrate immersed into the subphase for Y type and Z type dipping immersed into the subphase to a certain level and for X type dipping after zero point was settled; the level to be emerged was entered to the software program after solution is spread. The surface pressure where the solid like monolayer was obtained verified from the isotherm experiments defined as the target surface pressure where the deposition was done. After the evaporation of the solvent barrier start compression to form a monolayer and at the target surface pressure barriers tried to keep surface pressure constant and the dipping arm immersed or emerged the substrate in pursuant of the entered data and the dipping type. In the meantime, the monolayer and deposition isotherms were recorded and the value of transfer ratio (T.R.) was calculated by the program which defined as the ratio of the decreasing area of monolayer on surface of subphase to monolayer capped area of support.

T.R.: decreasing area of monolayer on surface of subphase / monolayer capped area of support

2.7. CTAB Isotherms Obtained on DI-Water and Aqueous Solution of PSS Sub-phases

To get experience about the system, in this study the monolayer of CTAB and gluing of these monolayers with PSS were studied. To observe the monolayer formation various spread volumes of CTAB, compression rates and PSS concentration of the subphase (DI-water) tried to be studied.

2.7.1. Effect of the Spread Volume of the CTAB Solution on the Isotherm of CTAB Monolayer

To get information about the monolayer formation of CTAB, the concentration of it was chosen as 0.07 mg/mL and at different compression rates the spread volume effects was studied.

2.7.2. Effect of the PSS Concentration of the Sub-phase on the Isotherm of CTAB Monolayer

0.1 mg/mL, 1.0 mg/mL, 5.0 mg/mL and 10 mg/mL aqueous solution of PSS were prepared and used as a sub-phase for the preparation of the isotherms of 0.07 mg/mL CTAB solution.

2.7.3. Effect of the PSS Concentration of the Sub-phase on the Hysteresis Curve of the CTAB monolayers

Hysteresis experiments at different PSS concentrations (0.1 mg/mL, 1.0 mg/mL, 5.0 mg/mL and 10 mg/mL) were studied and behaviour of the compression and expansion cycles were observed, and isotherm graphs and hysteresis experiments were obtained and results were given in the chapters 3.1.2 and 3.1.3.

2.8. Monolayers of CdSe QDs

In the preparation of CdSe QDs Langmuir films, CdSe QDs were synthesized. Since it is important to remove excess residues from the medium, to provide optimum surface pressure conditions during the film formation, an extensive cleaning procedure was applied. The synthesis of the CdSe QDs was described in the following section distinctly.

2.8.1. Synthesis of CdSe QDs

CdSe QDs were synthesized by modifying the procedures by using the thermal decomposition method [44, 46, 53]. Into the three necked 6.5 mg cadmium oxide (CdO), 0.6 mL oleic acid ($C_{18}H_{34}O_2$) and 5.0 mL of octadecene ($C_{18}H_{36}$) was added and heated to 225°C under magnetic stirring. After solution become clear and temperature reached to 225°C, 1.0 mL of selenium stock solution is added. Selenium stock solution was prepared at room temperature with adding 2.5 mL octadecene to 16.5 mg trioctylphosphine oxide and 15 mg selenium (Se). To obtain identical size distribution for this study all samples were removed after 60 seconds. The sample scheme of the synthesis set up was given in Figure 7.

To get rid of the side products and unreacted precursors two methods were studied. First one was extraction procedure performed with methanol and hexane in 1:1 (v/v) ratio [45, 54]. In this procedure, equal volumes of hexane and methanol were added to the synthesized quantum dot solution at room temperature. In this system, it was proposed that the unreacted precursors prefer the methanol phase and quantum dots prefers hexane phase [54]. After addition of hexane and methanol the solution was mixed and after certain time of equilibrium the separation of layers were observed, and the hexane phase was removed. Equal volumes of hexane and methanol is added to the removed hexane phase repeatedly and in each step hexane phase removed. This purification method has been continued until the layers are rapidly separated. After that with using rotary evaporator all the solvent removed, and quantum dots were dispersed in 6.0 mL chloroform ($CHCl_3$).

Second one is centrifuging with ethanol at 3000 rpm [39] QD solution was being centrifuged with ethanol and each time the excess ethanol as a supernatant was removed. After addition of ethanol to the quantum dot solution and it was mixed rapidly, then if the dispersion was observed within each other, the procedure was continued with the addition of ethanol. The same procedure repeated until there was no mixing of quantum dot and ethanol.

Figure 7 Synthesis set up of CdSe QDs

2.8.2. Optimization Studies of CdSe QDs Monolayers and Multilayers

In this part of the study, the effects of the compression ratio, the amount of CdSe QD that is spread on the sub-phase surface and adding stearic acid (SA) as a spacer were investigated in order to get an idea regarding the stability and quality of the monolayer.

2.8.2.1. Effect of Compression Rate on CdSe QDs Monolayers

For this optimization study, QDs solution spread on to the subphase and compressed at different compression rates while other parameters; temperature, concentration and volume were kept constant. For this aim, deionized water was used as a subphase and compression rate were adjusted in between 8-10-12 mm/min for each experiment and surface pressure versus area isotherms were recorded.

2.8.2.2. Effect of Spread Volume onto Subphase on CdSe QDs Monolayers

To clarify the effect of the volume of CdSe QDs on the isotherms of the QDs monolayers, various volumes (20 μL, 30 μL and 40 μL) of CdSe QDs solution were spread onto deionized water sub-phase. Experiments were done at constant concentration, temperature and compression rate conditions.

2.8.2.3. Effect of Usage of Stearic Acid as a Spacer on Monolayer Isotherm of CdSe Quantum Dots

In this part, to see the effect of adding stearic acid (SA) solution to quantum dot solution observed onto monolayer formation of quantum dot and deposition of monolayer. SA were chosen since it is used as reference material for LB system [55] .

2.8.2.4. Effect of Deposition Type on Transfer Ratio of CdSe QDs Monolayers

Hydrophilic and hydrophobic substrates were prepared as mentioned in section 2.5 and X and Z types of dippings that explained in section 1.2.3 were applied. As a consequence of the varying the deposition type of CdSe QDs monolayer onto the substrate, each time the transfer ratio was measured.

CHAPTER 3

RESULTS & DISCUSSION

In this work, Langmuir monolayers of CTAB and gluing technique by using PSS were studied. Optimization of experimental parameters were performed and stable monolayer of CTAB were obtained with gluing technique.

Trioctylphosphine oxide (TOPO) coated 2-4 nm CdSe QDs synthesized via thermal decomposition method and characterized with Fluorescence Spectroscopy and Transmission Electron Microscopy. After characterization of CdSe QDs Langmuir monolayers were obtained. The effect of spread volume of the solution and compression rate of the barriers on the formation of Langmuir monolayer of CdSe quantum dots were studied.

The deposition of the Langmuir monolayer of QDs were done on glass substrates and worked on the different deposition types (X type and Z type). The characterization of Langmuir Blodgett films was done with Confocal Microscopy and Transmission Electron Microscopy.

3.1. CTAB Isotherms Obtained on DI-Water and Aqueous Solution of PSS Sub-phases

In the introduction part, the Langmuir films of the surfactant were described briefly. The monolayers of the water-soluble surfactants can be obtained and deposited onto a substrate. However, to obtain a stable film for anionic or cationic surfactants they should interact with another material that provides the formation a complex between

the surfactant and another material. For this aim, addition of salts can be done to the subphase or mixed solutions of surfactants and fatty acids are reported in the literature [56, 60]. For this part of the study without complex formation CTAB monolayers were tried to be formed.

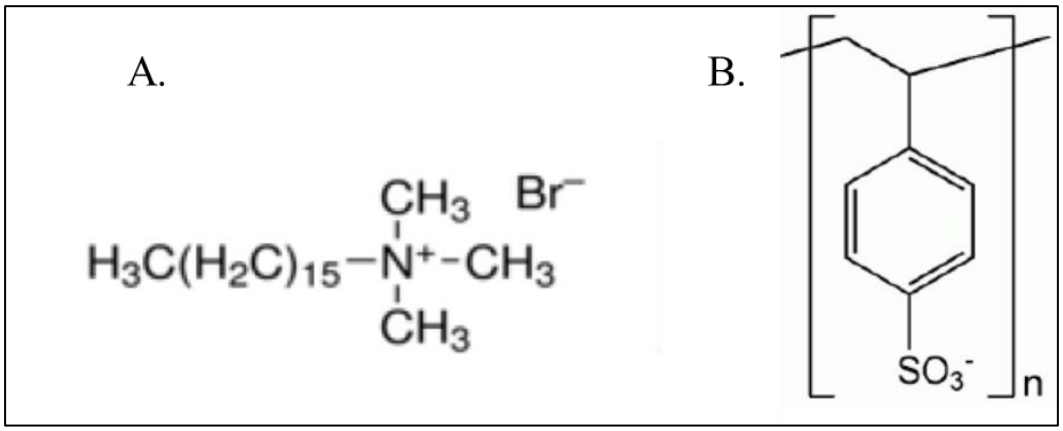

Figure 8 Structure of a) CTAB and b) PSS

At the beginning of the study cetyltrimethylammonium bromide (CTAB) (Figure 8a) isotherms studied since our beginning aim was to obtain a monolayer of silver nanoparticles. The π- MMA isotherms of CTAB on DI water studied. However, since we could not obtain CTAB isotherm at low concentration (0.07 mg/mL) thus gluing method was studied. In this method as mentioned introduction part, crosslinking provides a stable monolayer for surfactants on the air water interface. Therefore, PSS (Figure 8b) was used as gluing agent and comparison of the monolayer isotherms on DI H_2O and aqueous solution of PSS was used.

The temperature was adjusted as 20°C over the course of the experiments of CTAB and gluing method.

3.1.1. Effect of Spread Volume of the Solution on CTAB Isotherms

In order to investigate effect of spread volume of the CTAB solution onto the subphase, 0.07 mg/mL solution of CTAB in $CHCl_3$ was prepared. This concentration was decided according to the critical micelle concentration of CTAB that is between 0.34 – 0.36 mg/mL [61]. Moreover, the monolayer formation of CTAB was also studied before at the concentration of 0.15 mg/mL in $CHCl_3$ [55]. Therefore, we investigated the monolayer of CTAB at the concentration of 0.07 mg/mL.

40 µL and 50 µL of CTAB solution was spread onto the water subphase and compressed at the barrier moving rate of 8, 10 and 12 mm/min. As depicted in Figure 9 and Figure 10 at this concentration of CTAB we could not obtain any isotherm as we defined in section 1.2.2.3 on the water subphase.

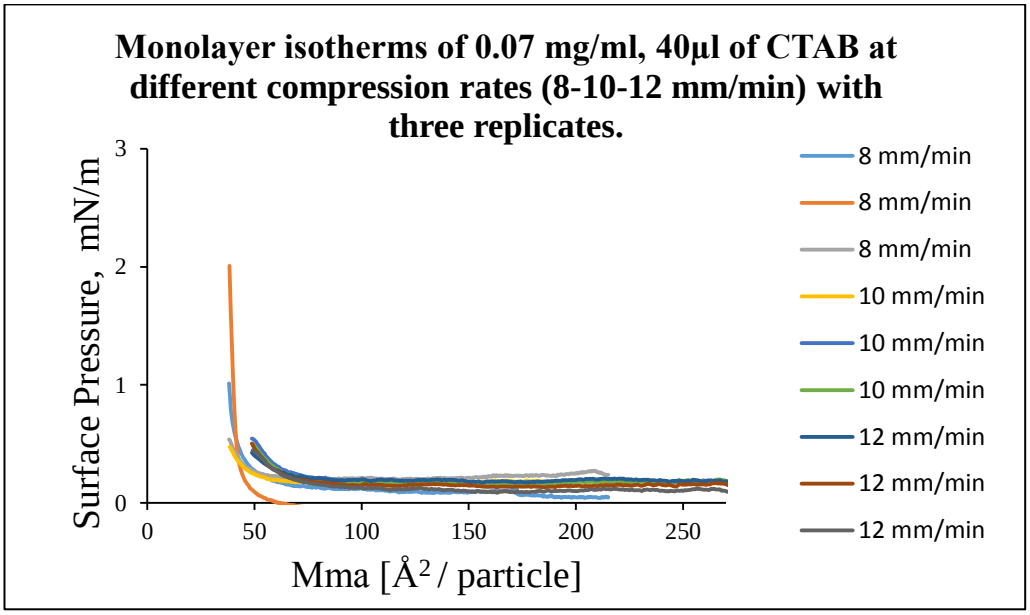

Figure 9 The isotherms of 40 µL of 0.07 mg/mL CTAB at three different compression rates (8-10-12 mm/min).

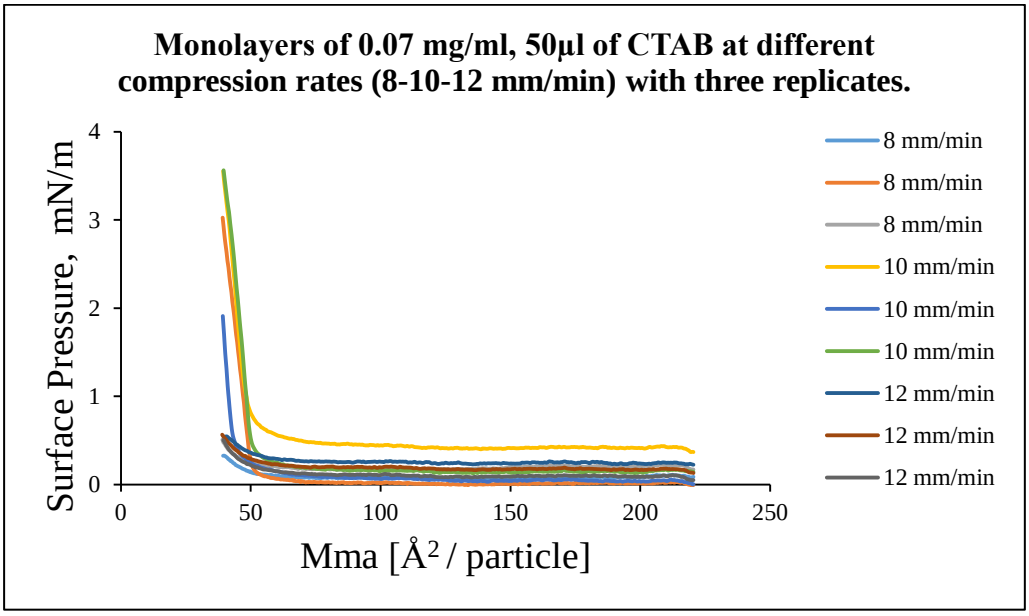

Figure 10 The isotherms of 50 µL of 0.07 mg/mL CTAB at three different compression rates (8-10-12 mm/min)

In these isotherms surface pressure remained almost zero or below 4 mN/m. This is due to the water solubility of the surfactant. After spreading the solution on to subphase the CTAB molecules show tendency to sink into the water subphase that is why we could not get a proper isotherm [62]. The volume for CTAB studies chosen as 50 µL due to the higher surface pressure compared to that in the 40 µL.

3.1.2. Effect of the PSS concentration on the CTAB isotherms

On deionized water since we could not get CTAB isotherm, as we mentioned before the gluing technique was applied. Therefore, aqueous solution of PSS was used as subphase. Moreover, to observe the effect of PSS concentration on CTAB isotherms at different concentrations of PSS, CTAB isotherms were obtained.

In Figure 11, 12 and 13 all isotherms for 50 µL of 0.07 mg/mL of CTAB solution on 0.1 mM, 1.0 mM, 5.0 mM and 10.0 mM PSS subphase at the compression rate of 8, 10 and 12 mm/min are shown, respectively.

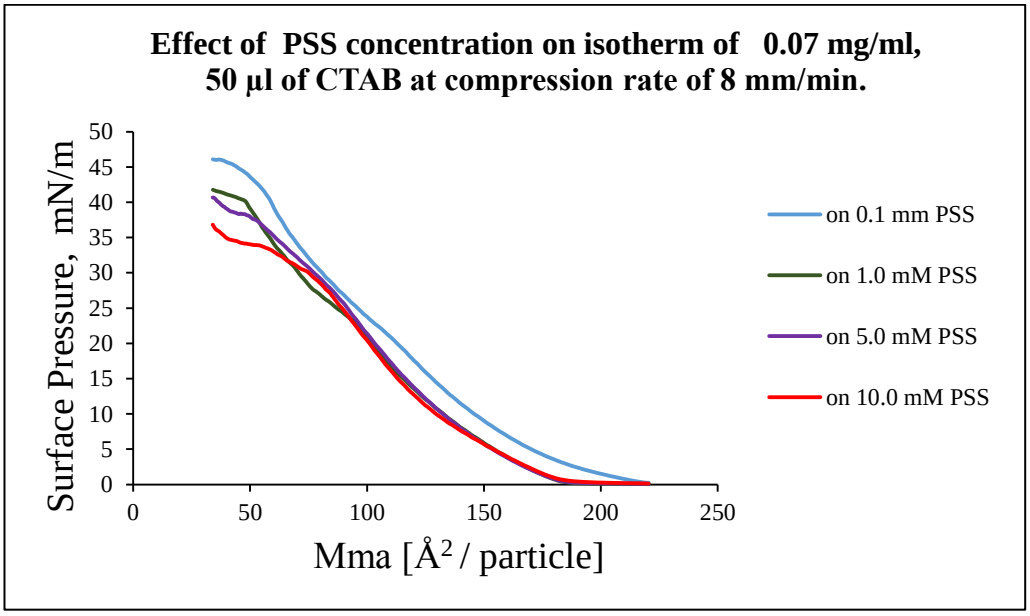

Figure 11 The isotherms of 50 µL of 0.07 mg/mL CTAB solution at a compression rate of 8 mm/min at various PSS concentrations, 0.1 mM, 1.0 mM, 5.0 mM and 10.0 mM

For all concentrations of PSS aqueous solution (0.1 mM, 1.0 mM, 5.0 mM and 10.0 mM) used as a sub-phase and the CTAB isotherms obtained were preferable compared to the ones obtained on pure DI water subphase. In these isotherms, we could observe the surface pressure increase up to 40 mN/m and the collapse point around 35-38 mN/m clearly. In this part of the study; due to the ionic crosslinking of the CTAB and PSS the monolayer was obtained on the air - water interface as explained in the Regen's studies [24, 63, 64] for the crosslinking interactions of the calix [6]-arene with the PSS and polymeric surfactants with polyacrylic acid (PAA) in order to increase the stability and robustness of the LB films. According to these given information, we could say that PSS probably indicates an ionic interaction with CTAB (0.07 mg/mL), which helped for the formation of a stable monolayer on the PSS aqueous solution sub phase.

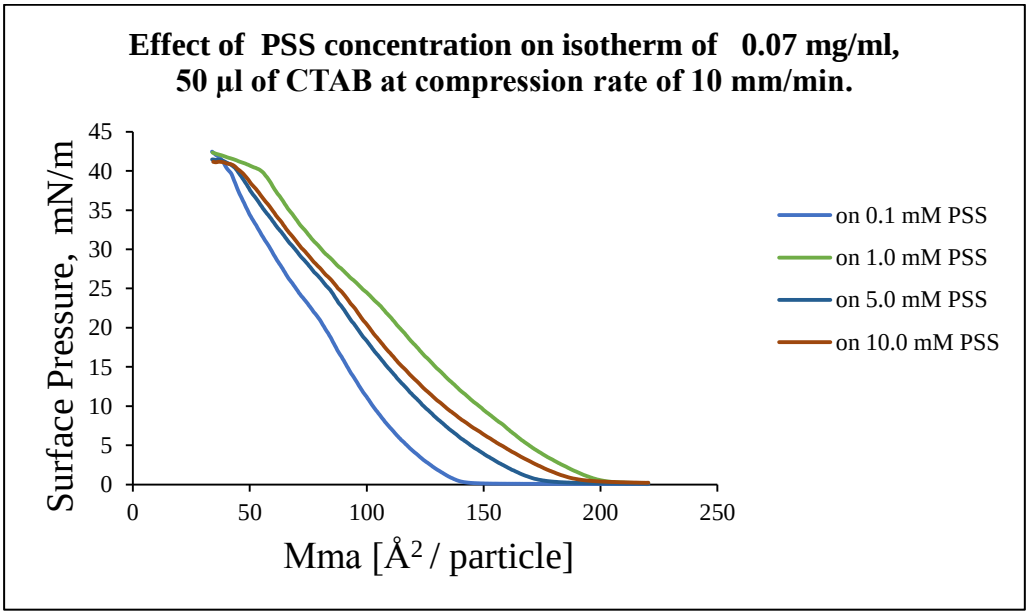

Figure 12 The isotherms of 50 µL of 0.07 mg/mL CTAB solution at a compression rate of 10 mm/min at various PSS concentrations, 0.1 mM, 1.0 mM, 5.0 mM and 10.0 mM

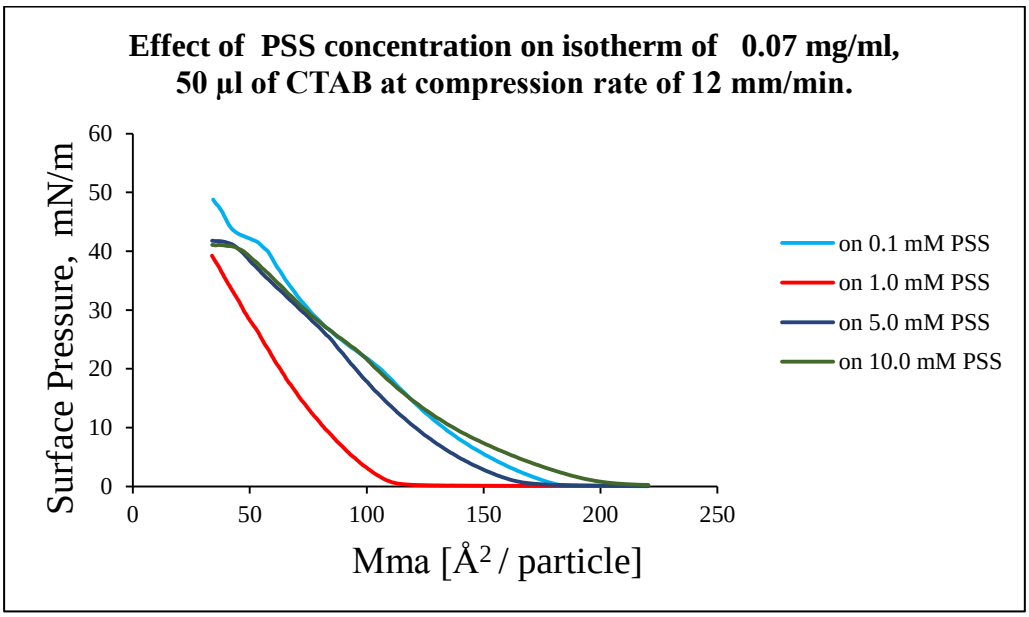

Figure 13 The isotherms of 50 µL of 0.07 mg/mL CTAB solution at a compression rate of 12 mm/min at various PSS concentrations, 0.1 mM, 1.0 mM, 5.0 mM and 10.0 mM

For various compression rate and PSS concentrations CTAB isotherms were obtained. In these isotherms, we were able to obtain the formation of CTAB monolayer with gas- liquid- solid phases as mentioned in the introduction part (1.2.2.3) and in Figure 14 as an example these phases were marked for the conditions of 0.07 mg/mL of 50 µl of CTAB solution with the compression rate of 12 mm/min on the aqueous solution of 5.0 mM. In this isotherm, region I indicates gaseous phase and with the increment of compression rate liquid phase is obtained that shown as region II. As a result of continuous compression molecules come close to each other and the slope change is observed, and solid phase is obtained, region III. The continuous compression results in the deformation of the monolayer which is named as collapse point and this point was observed as around 40 mN/m for this isotherm and indicated with region IV.

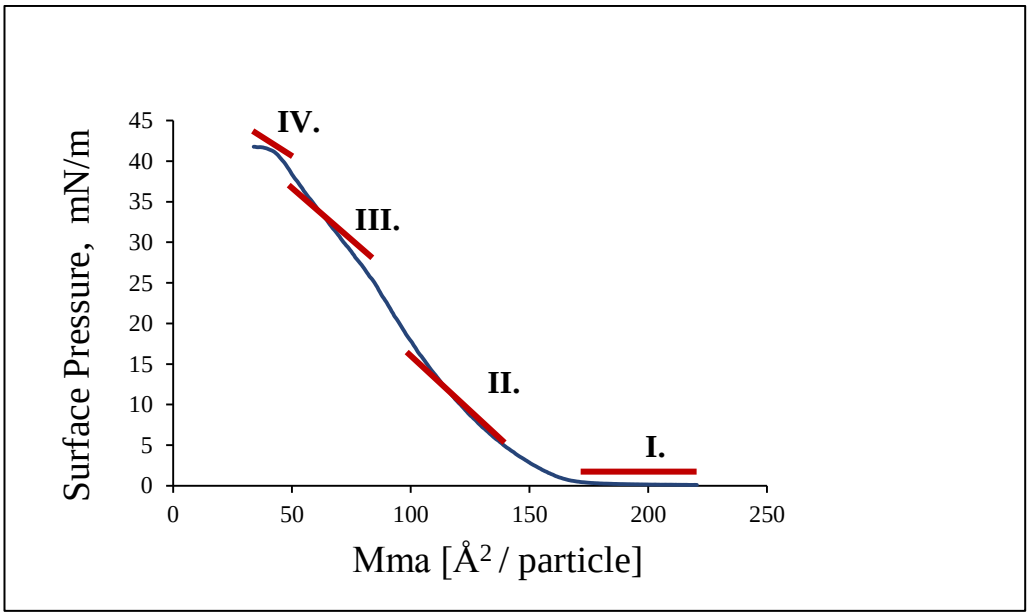

Figure 14 Example for the phases of the monolayer isotherm

The effect of the PSS concentration on the CTAB isotherms was explained in the next part with hysteresis experiments.

3.1.3. Effect of the PSS Concentration of the Sub-phase on the Hysteresis Curve of the CTAB Monolayers

The information about the stability of monolayers may be obtained throughout the hysteresis experiments that is the repeated compression and expansion cycles. During compression, due to the force that is applied by the moving barriers, the molecules come closer and start to form a monolayer and consequently phase transitions are observed. There are two different possibilities for an expansion cycle of a single layer. Molecules may either move away from each other following the same path as they come together they can pursue a different route during the expansion. The first signifies that molecules are compressed due to the movement of the barriers and are not inclined to interact with each other to form a single layer. Therefore; two isotherms that are completely superimposed to each other are observed for compression and expansion cycles. On the contrary for the second one if there is an interaction between the collateral molecules, the molecules indicate tendency to stay together. This ends up a different expansion isotherm compared to compression isotherm, which means molecules represent different behaviour during each compression and expansion cycle. This circumstance reveals that molecules do have hysteresis [65].

Therefore, to observe the effect of PSS concentration the conditions of 50 μL of 0.07 mg/mL CTAB solution on DI H_2O containing 0.1 mM, 1.0 mM, 5.0 mM and 10.0 mM PSS at the compression rate of 8, 10 and 12 mm/min were studied.

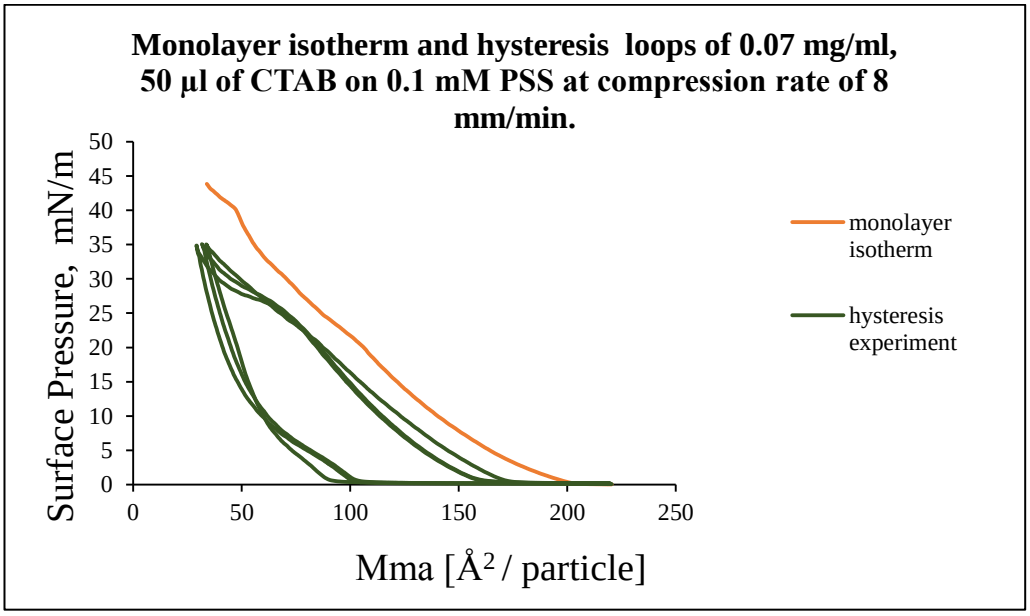

Figure 15 The monolayer and hysteresis isotherms of 50 µL of 0.07 mg/mL CTAB solution on DI H_2O containing 0.1 mM PSS at the compression rate of 8 mm/min at the target surface pressure of 35 mN/m

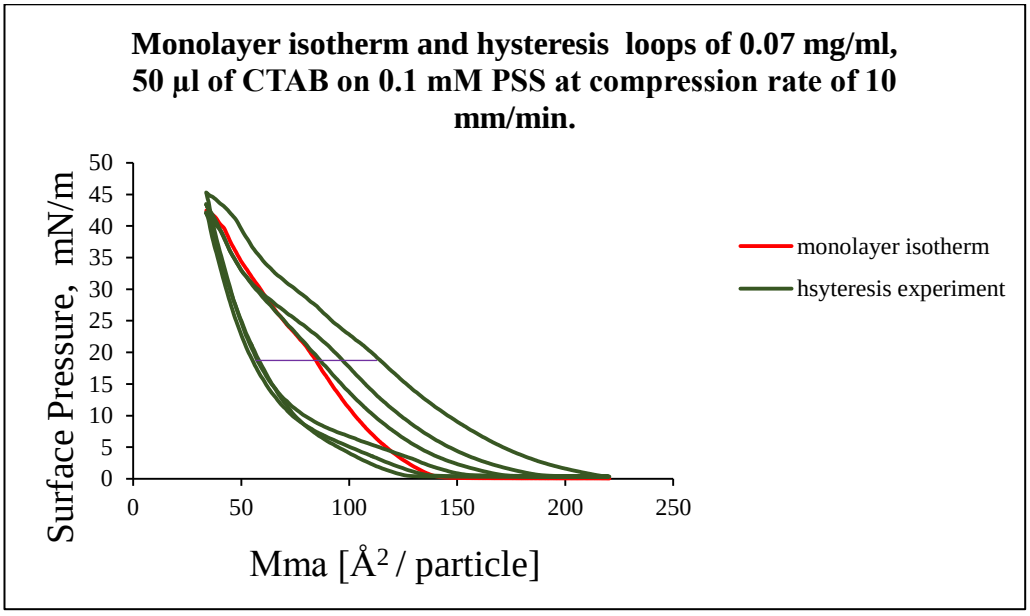

Figure 16 The monolayer and hysteresis isotherms of 50 µL of 0.07 mg/mL CTAB solution on DI H_2O containing 0.1 mM PSS at the compression rate of 10 mm/min at the target surface pressure of 45 mN/m

In Figures 15, 16 and 17 the monolayer and hysteresis isotherms of 50 µL of 0.07 mg/mL CTAB solution on DI H_2O containing 0.1 mM PSS at the compression rate of 8, 10 and 12 mm/min were shown. According to the data, with the compression rate of 12 mm/min hysteresis could not be observed as defined at the beginning of this section, the isotherms of compression and expansion cycle follow the same way. This could be the result of relatively high compression rate of the barriers that did not let to interaction of molecules of CTAB and molecules of PSS. Therefore, for other PSS concentrations, 1.0 mM, 5.0 mM and 10.0 mM compression rate was chosen as 10 mm/min for the hysteresis experiments.

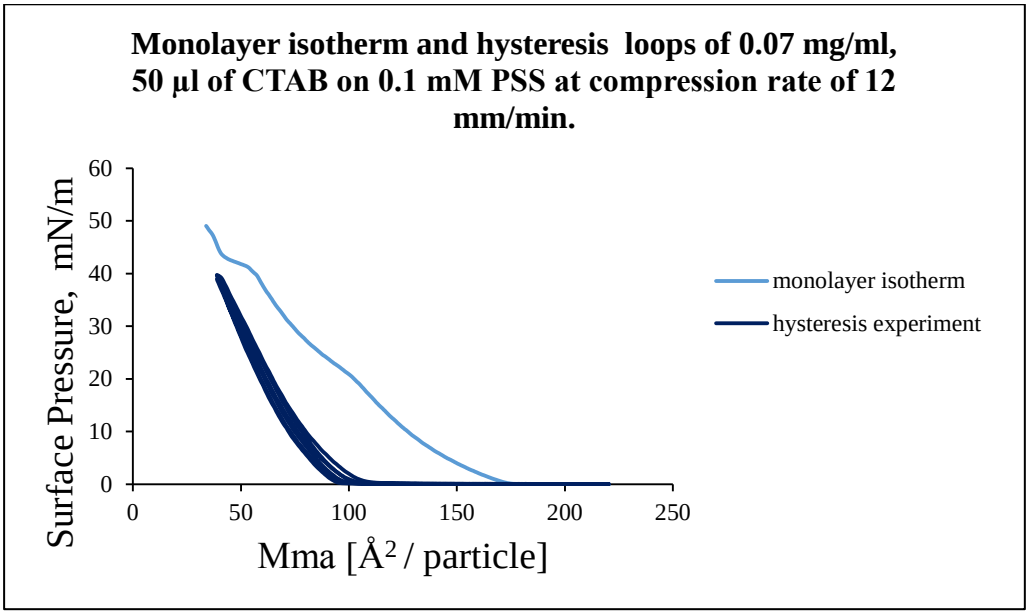

Figure 17 The monolayer and hysteresis isotherms of 50 µL of 0.07 mg/mL of CTAB solution on DI H_2O containing 0.1 mM PSS at the compression rate of 12 mm/min at the target surface pressure of 40 mN/m

Figure16, 18, 19 and 20 indicates the monolayer and hysteresis experiments of 50 µL of 0.07 mg/mL of CTAB in $CHCl_3$ at various PSS concentrations 0.1 mM, 1.0 mM, 5.0 mM and 10.0 mM.

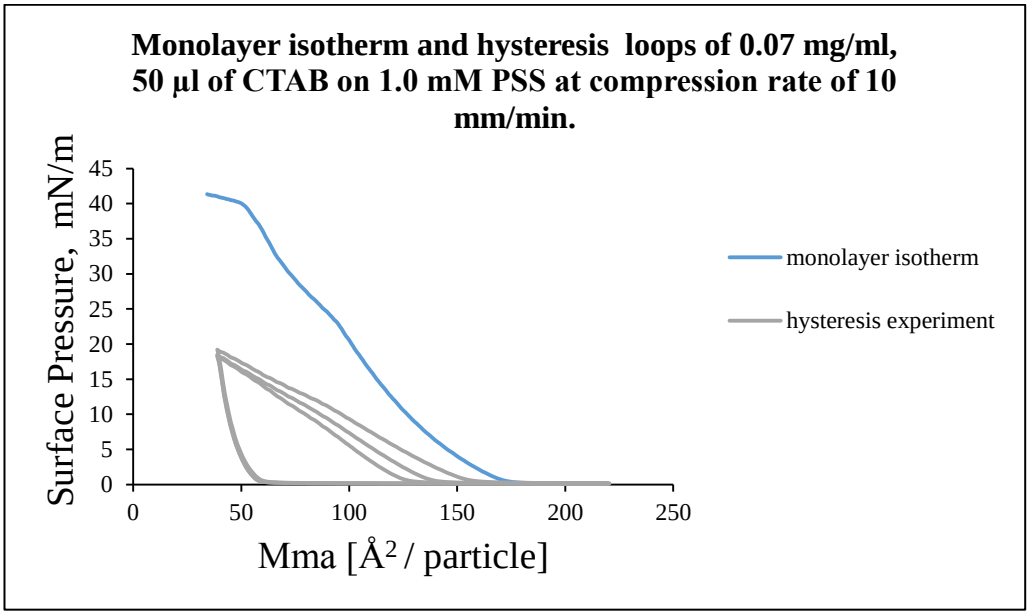

Figure 18 The monolayer and hysteresis isotherms of 50 µL of 0.07 mg/mL CTAB solution on DI H_2O containing 1.0 mM PSS at the compression rate of 10 mm/min at the target surface pressure of 20 mN/m

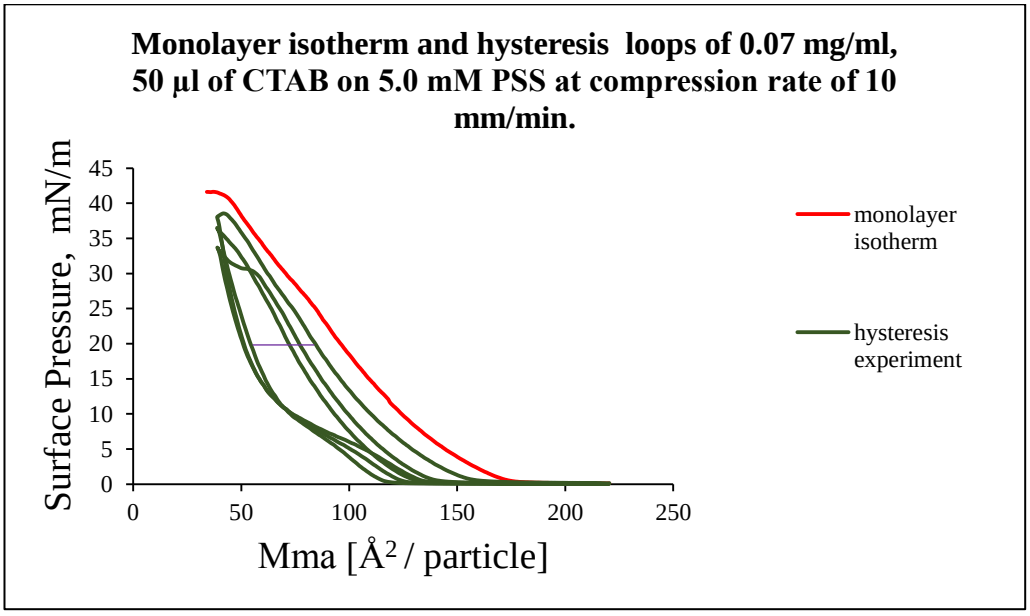

Figure 19 The monolayer and hysteresis isotherms of 50 µL of 0.07 mg/mL CTAB solution on DI H_2O containing 5.0 mM PSS at the compression rate of 10 mm/min at the target surface pressure of 40 mN/m

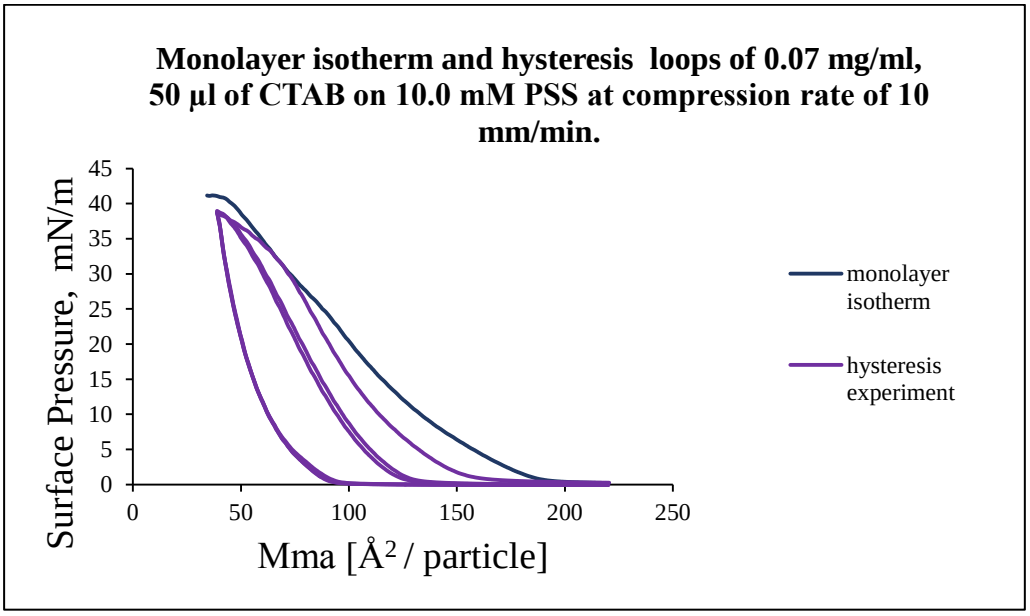

Figure 20 The monolayer and hysteresis isotherms of 50 µL 0.07 mg/mL of CTAB solution on DI H_2O containing 10.0 mM PSS at the compression rate of 10 mm/min at the target surface pressure of 40 mN/m

All the hysteresis experiments were done at the conditions of 50 µL of 0.07 mg/mL of CTAB with compression rate of barriers of 10 mm/min at 0.1 mM, 1.0 mM, 5.0 mM and 10.0 mM of PSS concentrations and were shown in Figures 16, 18, 19 and 20. In Figure 16, 18, 19 and 20; first compression cycles of the hysteresis are very close to isotherms of that conditions which again represents reproducibility of the monolayer formation at different time intervals which means with the same conditions we could get same isotherm attitude on different days. When the way of the compression and expansion cycles for each hysteresis experiment compared, isotherms' attitude indicates the interaction of the CTAB and PSS molecules. This interaction is understood from the path difference of the compression and expansion cycles. In Figures16, 18, 19, and 20 the space that is horizontal length the between compression and expansion cycles indicated as an example in Figure 16 and 19 with a purple line was smaller than the that of Figure 16. This is the result of the more interaction of the CTAB and PSS molecules compared to others. This interaction was mentioned in the Regen's study the space between the compression and expansion cycle for 0.1 M is the result of the viscous attitude of the molecules that is they form

viscous monolayers. This viscous attitude as explained in terms of competition of molecules to interact with each other. At higher concentration of PSS (1.0 mM, 5.0 mM and 10.0 mM) the extent of interaction between CTAB and PSS is lower than due to the presence of more polymer chains that can compete with each other to interact with CTAB compared to that of the low concentration of PSS (0.1 mM) [63].

For this part of the study, CTAB monolayers that we could not obtain on DI H_2O subphase were obtained on the PSS containing subphase successfully.

For further studies of silver nanoparticles as mentioned in section 1.4, deposition parameters must be optimized to transfer of silver nanoparticles monolayer onto a solid substrate and get a glued film of CTAB and PSS. Yet, in the continuous part of the study; we decided to prepare LB thin films of cadmium selenide (CdSe) quantum dots instead of silver nanoparticles to see the emission of the quantum dots that were arranged on the surface of the subphase by using UV light in a cheaper way of characterization method. Therefore, the optimization studies related to silver nanoparticles were not scope of this study since we desired to study on fluorescence material, CdSe quantum dots.

3.2.Synthesis of CdSe Quantum Dots

The synthesis of CdSe quantum dots were done by using CdO and Se as a precursor, TOPO and oleic acid as surfactant and octadecene as solvent with thermal decomposition method as mentioned in section 2.8.1. In order to characterize synthesized CdSe quantum dots; fluorescence spectrometer, hand held UV lamp and transmission electron microscopy were used.

3.2.1. Hand-Held UV lamp

The simple characterization was done with hand-held UV lamp. The colour observation of the QDs under sunlight and their specific excitation wavelengths also give information about the quantum dots. QD solution prepared was dropped onto a

glass substrate and its fluorescence was observed under both sunlight and hand-held UV lamp. Each time the fluorescence of a blank glass substrate measured for comparison. The UV lamp works at 254 nm and 365 nm. In Figure 21, the colour difference of quantum dots under UV lamp (354 nm) and under sun light are presented. The excitation wavelength of quantum dot was 400 nm [53]. Therefore, 365 nm wavelength was used.

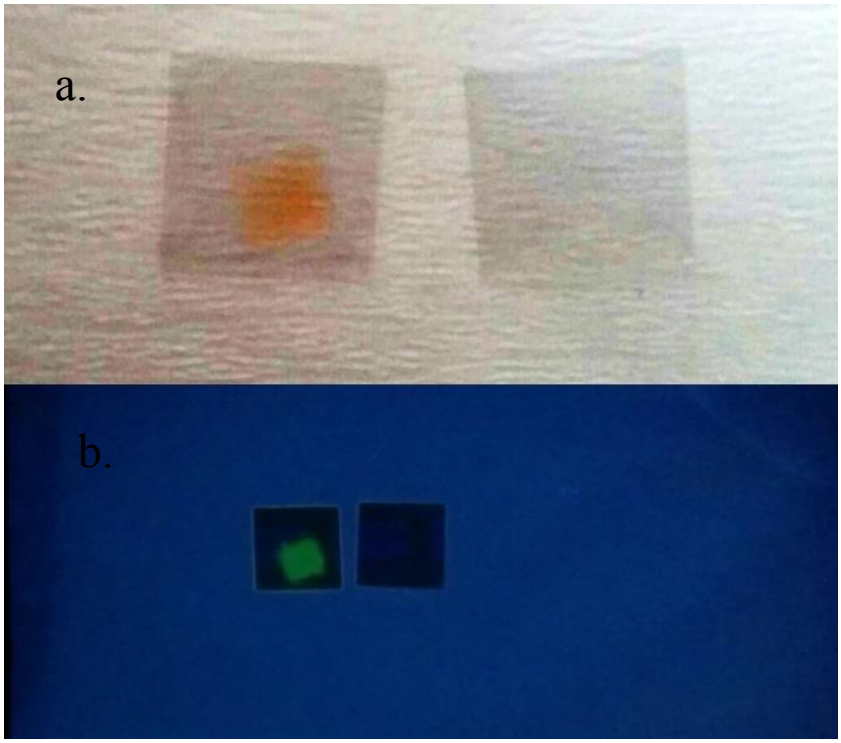

Figure 21 Images of the CdSe quantum dot solution on the glass substrate a) under sunlight b) under hand held UV lamp at a wavelength of 365 nm

3.2.2. Fluorescence Spectrometer

Fluorescence measurement is a very practical way of understanding the success of QD nanoparticle synthesis. Wide wavelength range (400 nm to 700 nm) measurements of CdSe QDs colloidal solution were performed using spectrofluorometer. Emission spectra of the CdSe QDs not only prove their existence in the solution but also give information about the approximate size of the quantum

dots. As all known [66] quantum dots have quantized energy levels that will give out different wavelength of light depending on how big they are. The biggest quantum dots emit light having lowest frequencies whereas the smallest dots emit light at higher frequencies. Boatman and her colleagues relates the size of the QD's to the emission wavelength of the fluorescence spectrum [53]. Therefore, once the emission spectrum is taken the size of the QD can be forecasted easily. The fluorescence emission spectrum of quantum dots in octadecene after synthesis without any purification was given in Figure 22.

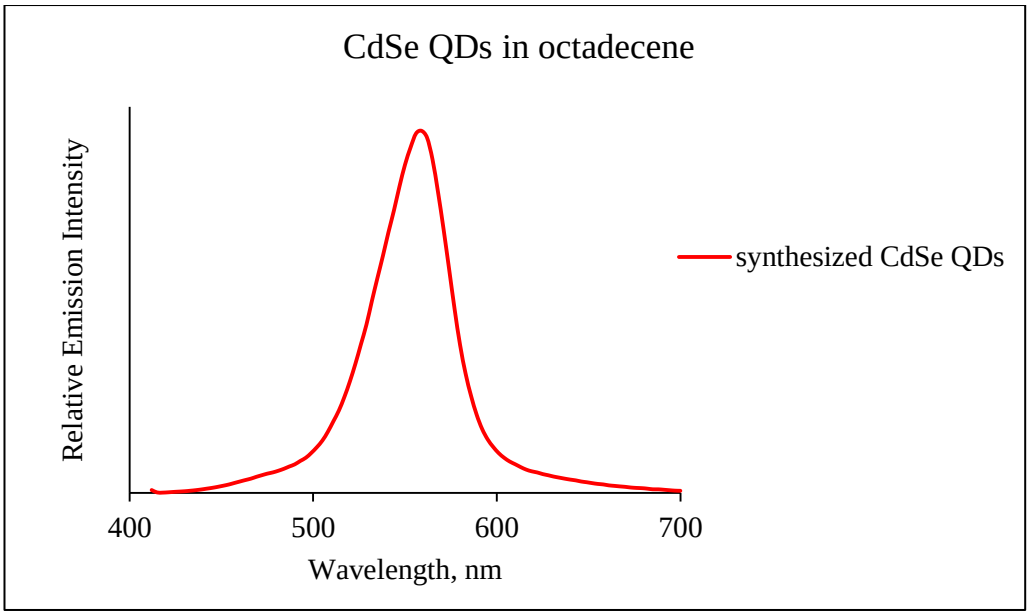

Figure 22 The emission spectrum of synthesized CdSe QDs before purification steps

As can be seen Figure 22, the emission wavelength of CdSe quantum dots at the excitation wavelength of 400 nm [53] was at 558 nm. According to this emission wavelength of quantum dots the synthesized particles are in the range of 2-4 nm [53].

For characterization of CdSe quantum dots two purification methods were studied as mentioned in section 2.8.1.

Firstly, methanol and hexane extraction was used. According to the fluorescence spectrum of methanol and hexane phase we already obtained the existence of quantum dots. Yet, although we could read emission intensity of quantum dots in hexane phase as will be mentioned in section 3.2.3, this purification method was not successful.

For the extraction procedure after each washing step with methanol and hexane their fluorescence intensities were measured and summarized below. In this extraction step each time equal volumes of methanol and hexane were added to the synthesized quantum dot solution. After we observed clear separation of the hexane and methanol phases, the methanol phase was removed. To the remained hexane phase again equal volumes of hexane and methanol were added and extraction procedure was applied repetitively.

In section 2.8.1 it was proposed that in this extraction method quantum dots prefers hexane phase and other unreacted precursors prefers methanol phase. As a result, we did not observe any quantum dots emission at 558 nm in methanol phase for each purification step. Therefore, only one emission spectrum of methanol phase was given in Figure 23. Inset figure also indicated that quantum dots prefers hexane phase.

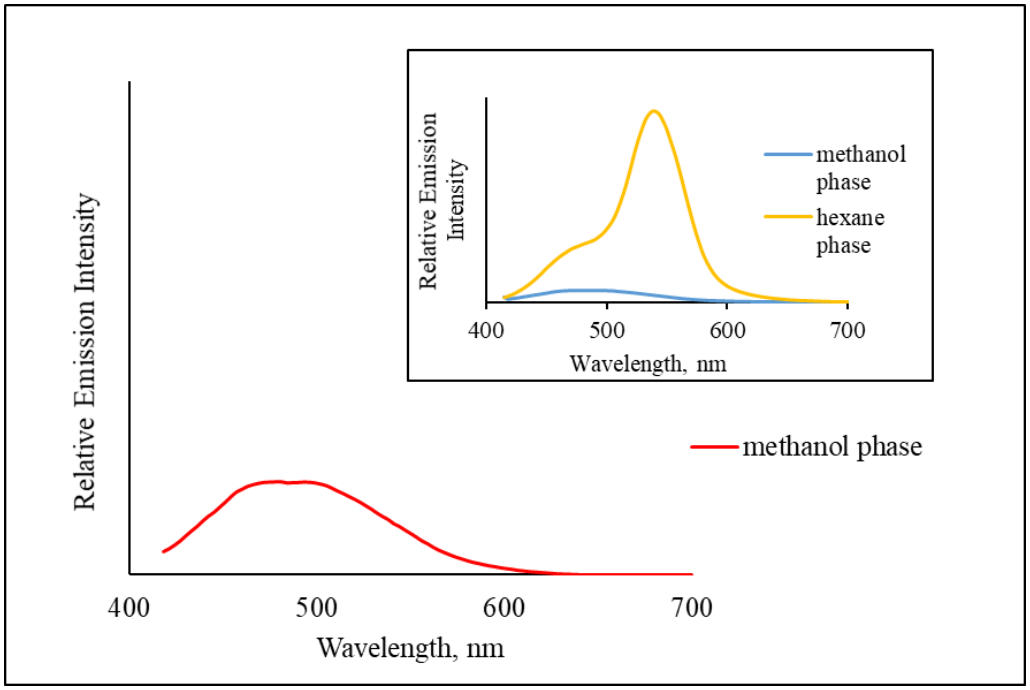

Figure 23 The emission spectrum of methanol phase in the course of purification of CdSe QDs and in the (inset comparison of emission spectrum of methanol and hexane phase)

Figure 24 indicates the emission spectra of CdSe quantum dots during purification step by using extraction method. Figures 24 a, b, c, d and e indicates the emission spectra of hexane phases of each extraction step.

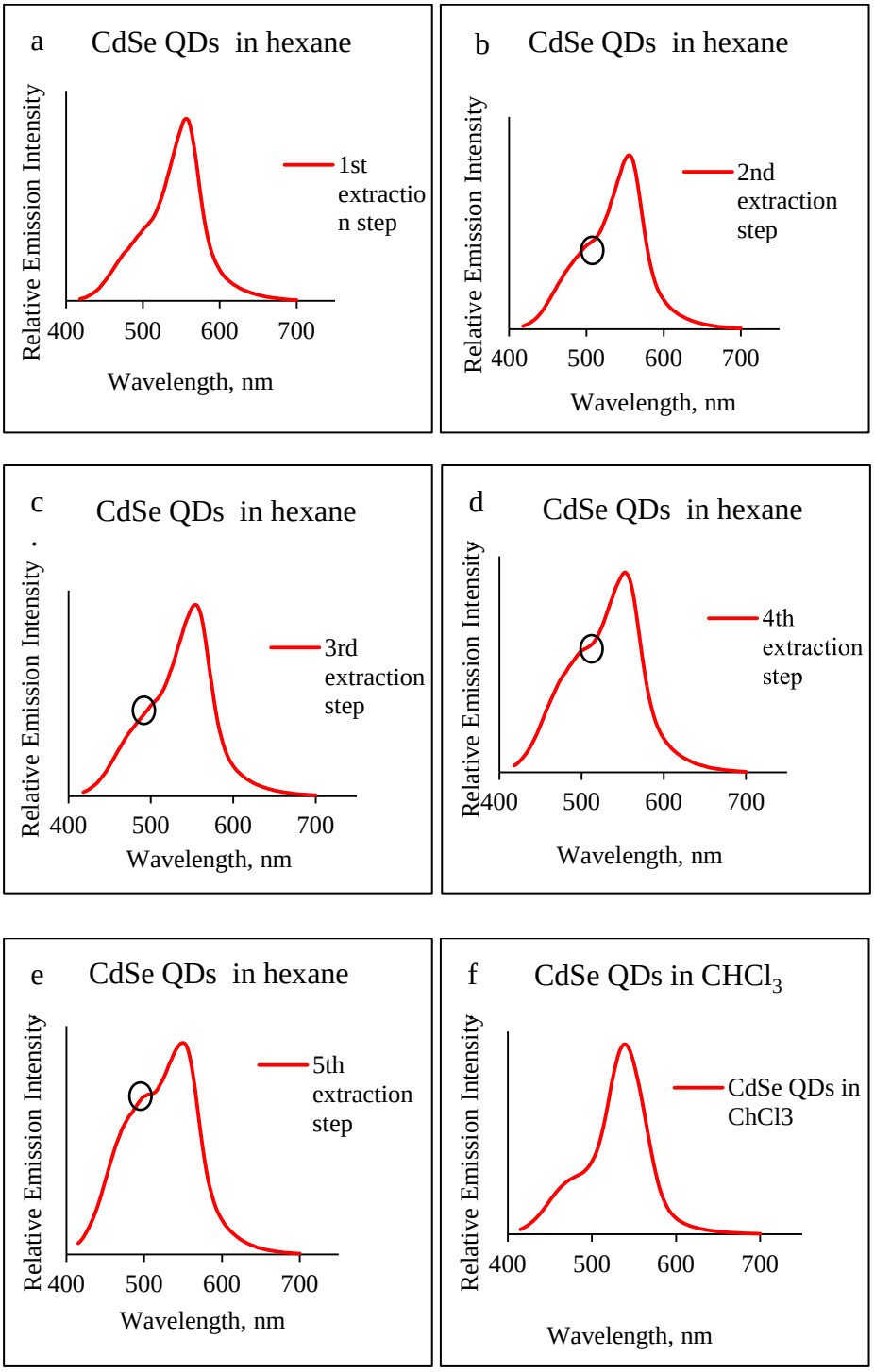

Figure 24 The summary of emission spectra of CdSe QDs that purified with extraction method

As stated in the literature the emission wavelength of this shoulder shows a blue shift as the size of quantum dots decreases [53]. In our studies at each step of the extraction procedure we also observed the shoulder formation that is shown with

black circle in each extraction step and the shifting of the peak point of this shoulder to shorter wavelength due to the size dependent separation of the particles. This step is shown in Figure 24 a to e.

At the end of the purification process, quantum dots were dispersed in chloroform as a mostly used solvent in Langmuir Blodgett technique due to its immiscibility in water and the emission spectrum is given in Figure 24 f and the clear emission intensity was read.

As a second purification method quantum dots were centrifuged with ethanol and the emission spectrum is given in Figure 25. According to this spectrum, purification was done and proved with TEM image as shown in the next section.

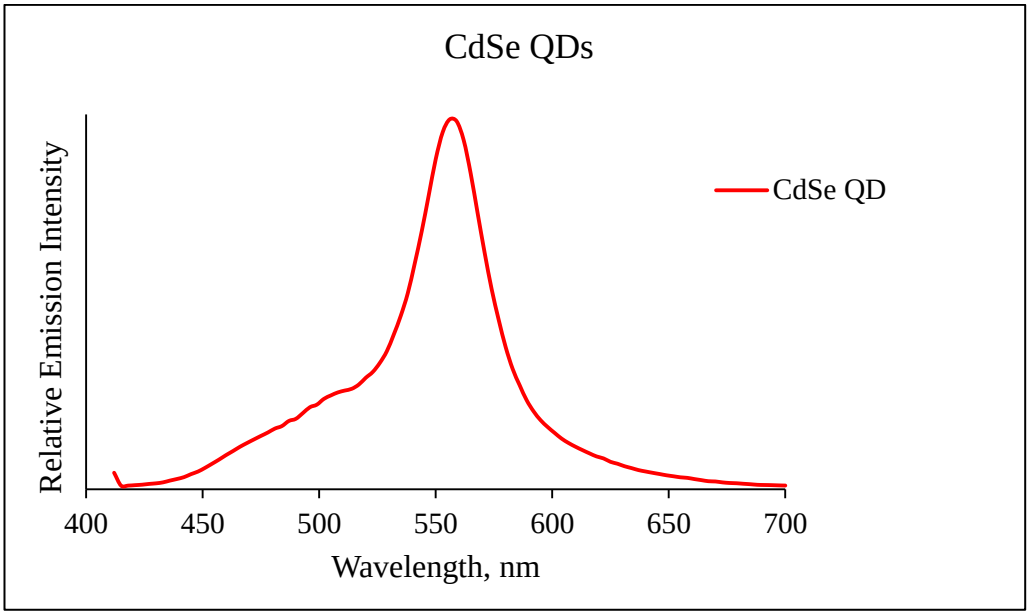

Figure 25 The emission spectrum of CdSe QDs after washing with ethanol and dispersed in $CHCl_3$

3.2.3. Morphology and Distributions

The image of the dilute QD solution under Transmission Electron Microscopy gives information about the morphology, size and homogeneity about their size distribution.

For the washing procedure with extraction although the emission intensities give information about the CdSe quantum dots were synthesized; TEM images indicates that this washing method was not successful. In Figure 26, TEM images of quantum dots that were purified with extraction method were indicated. As could be seen from the image depending on the washing procedure micelle formation was observed around the quantum dots. Moreover, from the images we could not talk about the homogeneity of the particles since agglomeration was observed. Therefore, throughout the TEM image of quantum dots that were purified with the extraction procedure was not favourable to use for experiments.

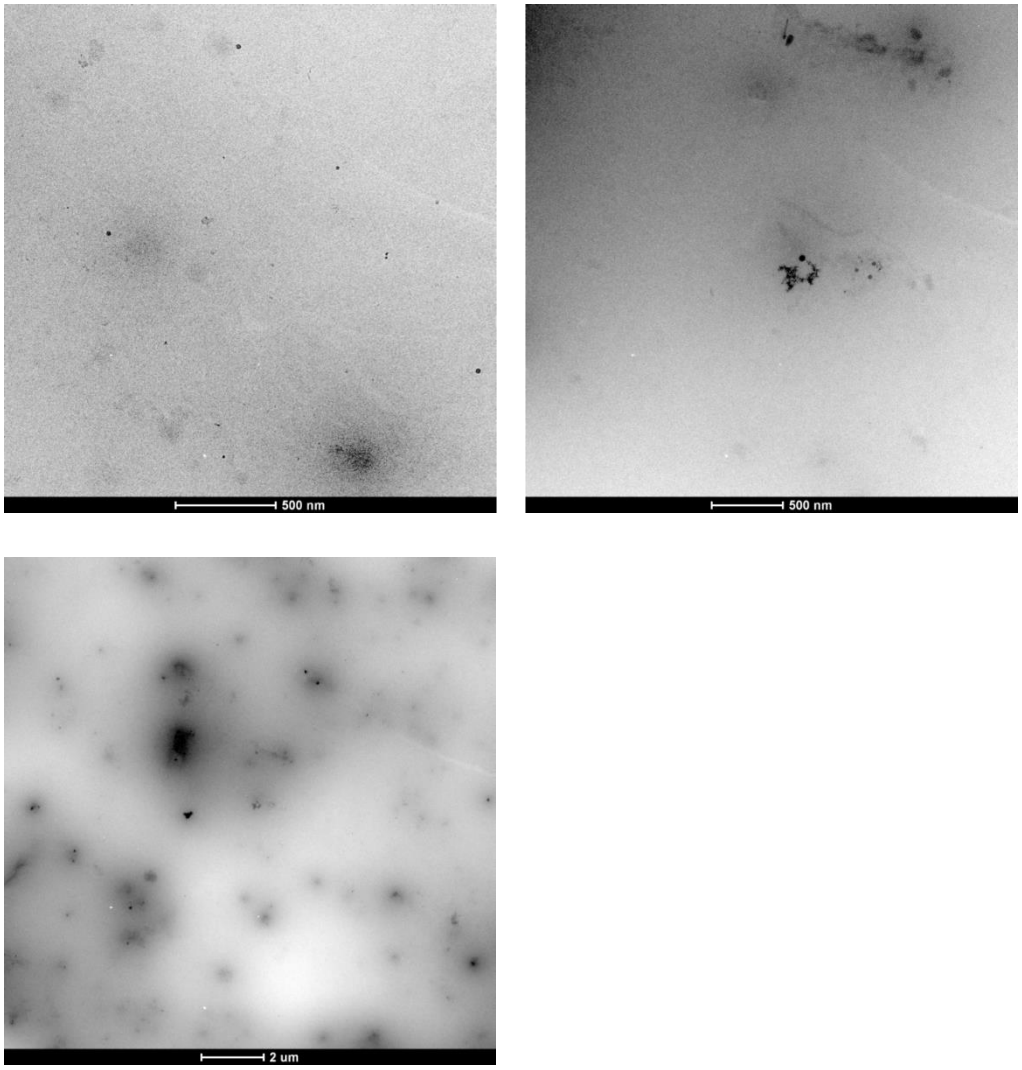

Figure 26 TEM images of that CdSe QD solution that tried to be purified with extraction method

For the purification of quantum dots centrifuging with ethanol was used as a second method as mentioned in section 2.8.1. As can be seen from Figure 27, with corresponding their emission wavelength (558 nm), quantum dots are 2-4 nm in size and their size distribution graph indicates the size distribution of the synthesized CdSe quantum dots. According to this graph about 70 particles are between the 2-4 nm scale per 100 particles (Figure 27b). Although fluorescence spectra obtained with extraction method and centrifuging with ethanol were similar to each other, TEM

image of ethanol washed quantum dots indicated no agglomeration as shown in Figure 27a.

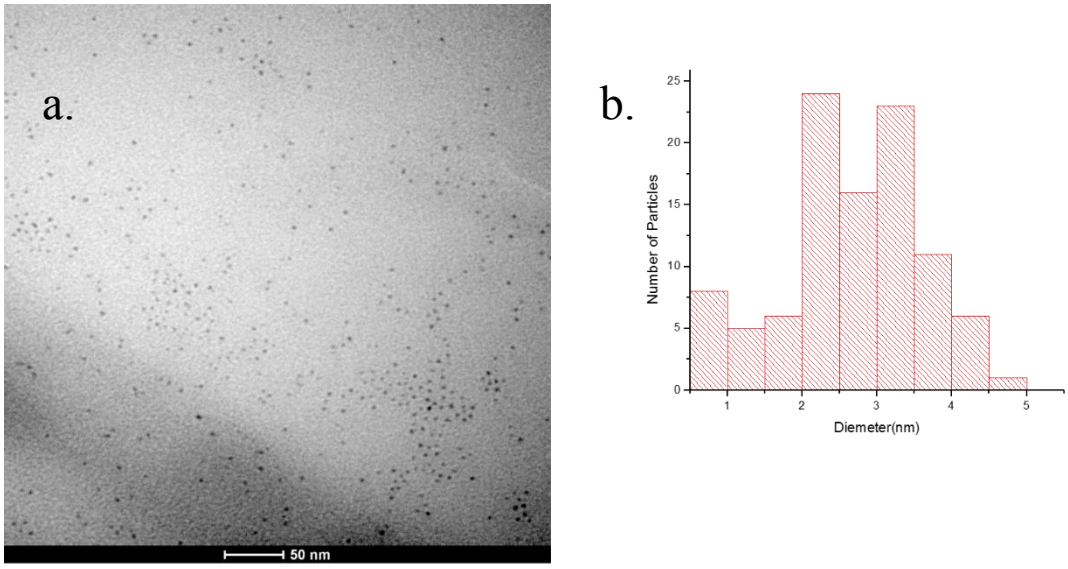

Figure 27 a) TEM image and b) size distribution graph of CdSe quantum dots that were purified with centrifuging with ethanol

3.3. Surface Modification of Glass Substrates

Before starting dipping experiments, glass substrates were being rendered as hydrophilic or hydrophobic depending on the desired experiments. After treatment with base piranha solution the surface of the glass substrates was hydrophilic. Hydrophobic substrates were obtained after treating them with CTMS solution. Following each treatment, the surface of the glass substrate was characterized with contact angle measurement. The contact angles for base piranha treated glass substrates and CTMS treated glass substrates were measured around 27° and 105°, respectively. The results were corresponding to the contact angle values generally obtained from the hydrophilic and the hydrophobic surfaces. The appearances of the water droplet on hydrophilic and hydrophobic surfaces are presented in Figure 28.

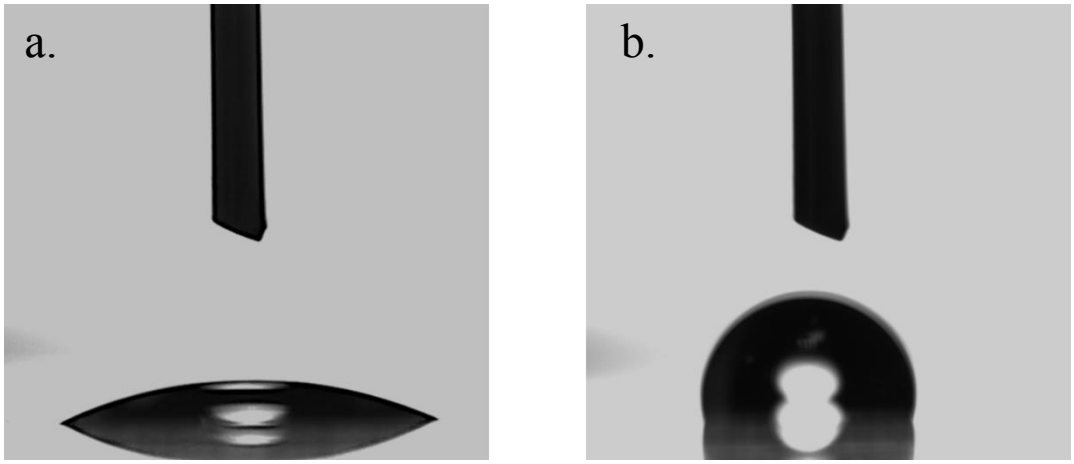

Figure 28 The appearances of the water droplet on a) hydrophilic and b) hydrophobic surfaces respectively

3.4. Optimization Studies of CdSe Quantum Dots Monolayer

Monolayer of CdSe QD's were being prepared on water subphase. Several Langmuir isotherms were constructed to optimize the volume of CdSe QD's solution to be compression rate of the barriers and injected volume in order to establish a stable LB films of QD's. Both monolayer and deposition experiments of CdSe QDs were carried out at 23 °C.

3.4.1. Effect of Compression Rate on CdSe Quantum Dot Monolayer

In order to observe the effect of compression rate on the formation of the monolayer of CdSe quantum dot; 40 μL of CdSe solution was being spread onto subphase and after the evaporation of the solvent compression was started. In Figure 29, monolayer isotherms of 40 μL of CdSe solution at the compression rate of 8 mm/min that were taken at two different days were shown. Moreover, In Figure 30, these isotherms were superimposed and the reproducibility of these monolayers were shown. This means at the same conditions but different time intervals we could take the same monolayer isotherm attitude.

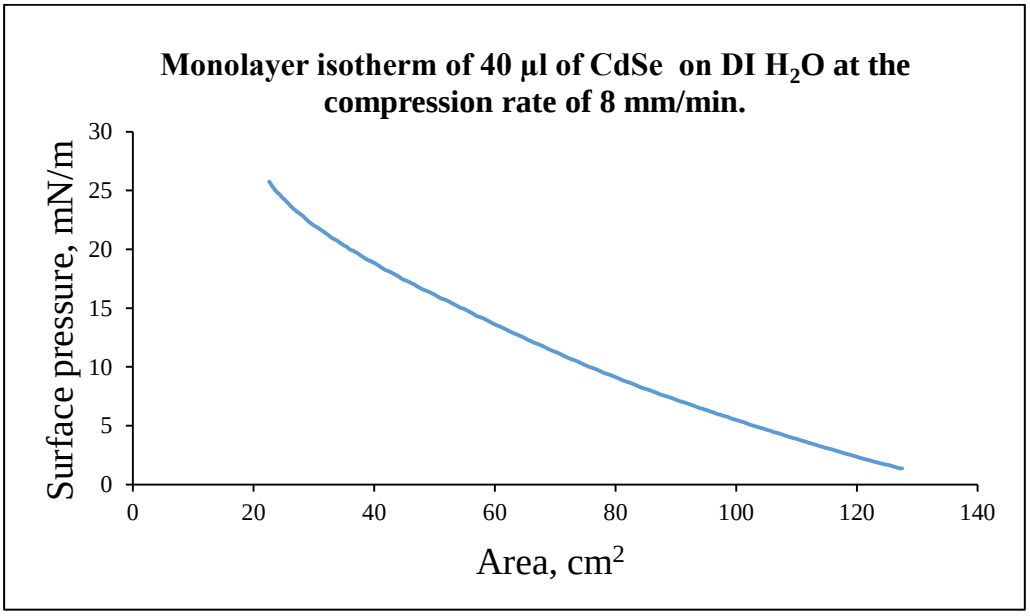

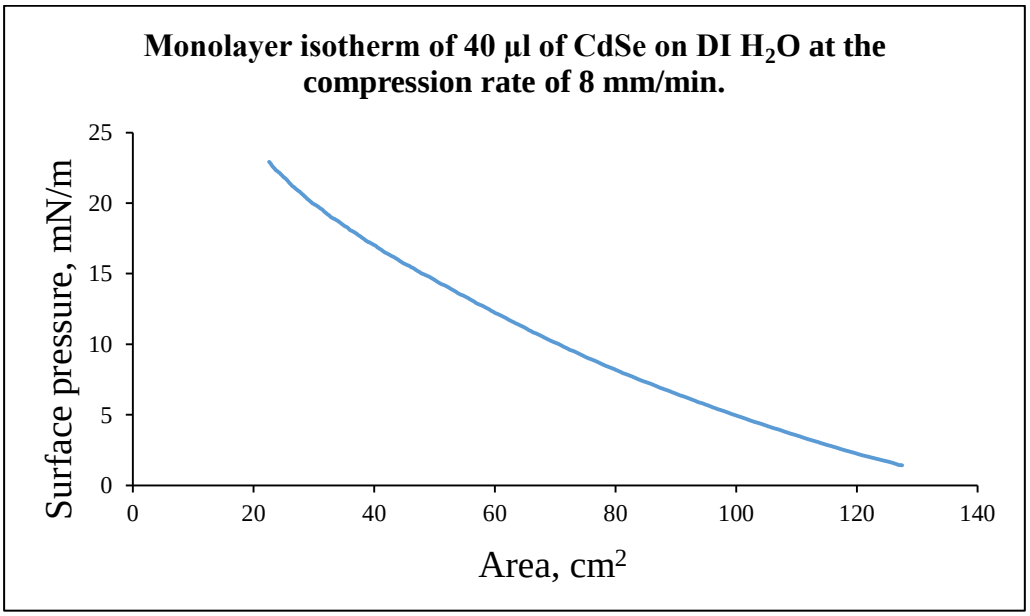

Figure 29 Monolayer isotherms of 40 µL of quantum dot solution compressed at the barrier rate of 8 mm/min that were taken on different days

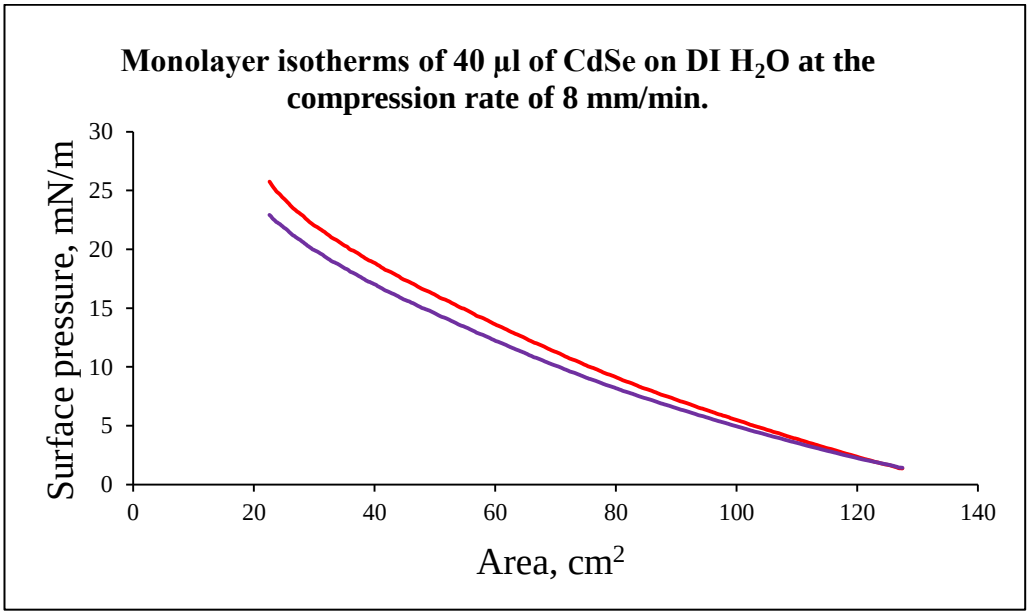

Figure 30 Isotherms of 40 µL of quantum dot solution compressed at the compression barrier rate of 8 mm/min

For other compression rates of 10 mm/min and 12 mm/min monolayer isotherms were taken. To see the effect of the compression rate on the monolayer formation of CdSe quantum dots, monolayer isotherms that were taken at 8 mm/min, 10 mm/min and 12 mm/min and in Figure 31 these isotherms were superimposed. As can be seen from isotherms, at different compression rates, the monolayer isotherms of 40 µL of CdSe QD solution follow the same way. Therefore, compression rate has no effect on the monolayer formation of 40 µL of CdSe QD solution as shown in Figure 31.

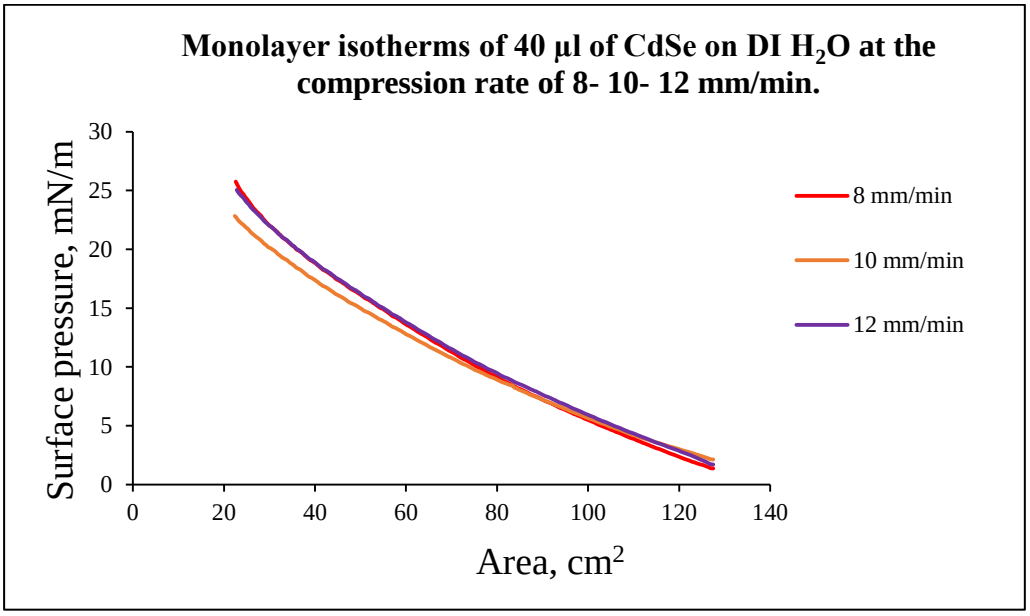

Figure 31 The monolayer isotherms of 40 µL of the CdSe quantum dot solution at the compression rate of 8, 10, 12 mm/min respectively

3.4.2. Effect of Spread Volume of QD Solution on CdSe Quantum Dot Monolayer

With the aim of observing effect of spread volume of QD solution on CdSe quantum dot monolayer 20 µL, 30 µL and 40 µL of CdSe solution spread onto deionized water and isotherms were taken at the compression rate of 10 mm/min.

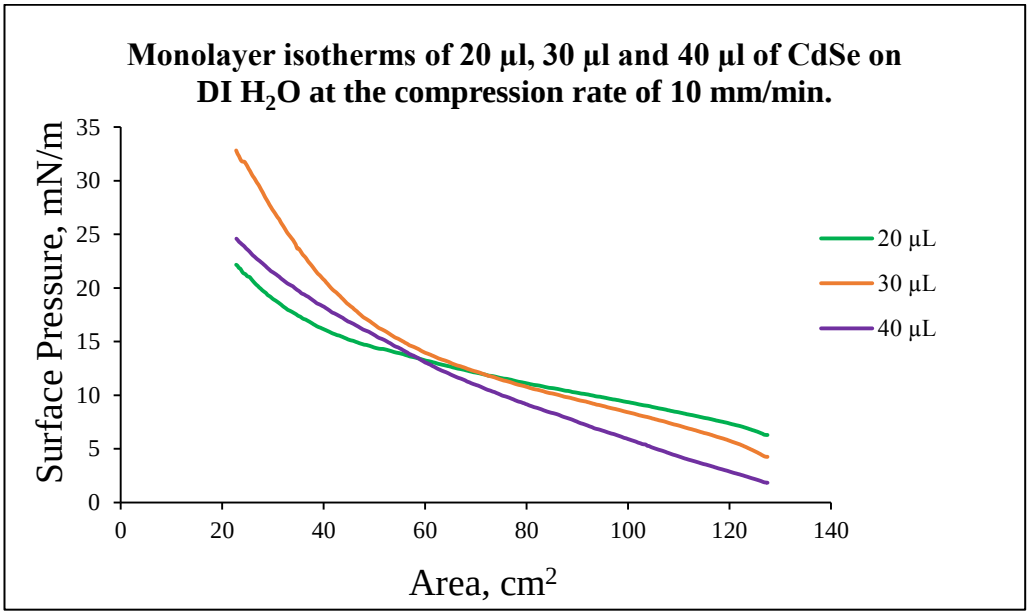

Figure 32 The monolayer isotherms of 20 µL, 30 µL and 40 µL of the CdSe quantum dot solution at the compression rate of 10 mm/min respectively

As depicted in Figure 32, the monolayer isotherm of 30 µL of CdSe quantum dot solution has the highest surface pressure when compression was finished. Since we could not observe collapse point that was defined in sections 1.2.2.3 and 2.4 for isotherms of CdSe quantum dots it might be concluded that with the highest surface pressure we were closer to the collapse point compared to other volume values. Therefore, for the deposition onto glass substrates was done with this volume value that will be mentioned in the section 3.6.1.

3.5. Study of Cadmium Selenide Quantum Dot – Stearic Acid Mixed Solution Isotherms

A dense control over the interparticle spacing is necessary that may be provided by incorporating an amphiphilic molecule as an intermediate. The Langmuir monolayer behaviour of CdSe quantum dots in the presence of stearic acid (SA) molecules was studied to provide an enhancement in the stability of the LB layer of QD's. In these studies, SA has improved the diffusion properties of quantum dots on the subphase

and were enabled the stable monolayer formation at the air-water interface [67]. Therefore, 120 µL of 1 mg/mL (w/v) SA solution was mixed with 240 µL CdSe quantum dot solution just before spreading onto the sub-phase. 20 µL of this mixture solution spread onto the subphase and monolayer formation was observed at the compression rate of 10 mm/min.

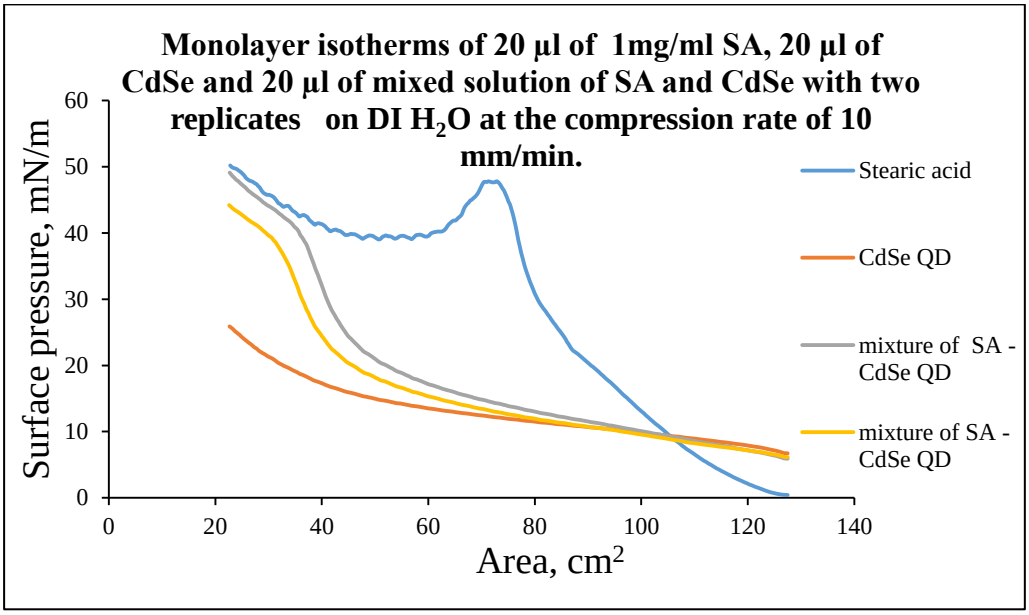

Figure 33 The isotherms of 1 mg/mL 20 µL of stearic acid solution, 20 µL of CdSe quantum dot solution and the isotherm of mixture of 20 µL of stearic acid and quantum dot solution with two replicates at the same compression rate, 10 mm/min

When we looked SA isotherm in Figure 33, we could observe collapse point. In detail, for SA isotherm, gaseous phase was observed a little bit and with continuous compression liquid phase and collapse point was observed at surface pressure around 50 mN/m respectively. When we looked at the monolayer isotherm of CdSe quantum dot solution (the red one) we could not observe collapse point where the monolayer formation already finished, and deformation of monolayer is observed as mentioned in section 1.2.2.3 and 2.4. Moreover, as could be seen from Figure 33 SA provided observing the phase transition for the monolayer isotherm of mixed solution of SA and CdSe quantum. While we could not observe an isotherm with phase transition for only quantum dot solution; the mixture of the SA and quantum dot solution

indicates a collapse point around 40 mN/m. Since we observed collapse point in this mixture isotherms we also performed deposition experiments. These experiments are in the section 3.6.1.

3.6. Transfer of CdSe QDs Monolayer onto a Solid Substrate

Langmuir monolayers of CdSe quantum dots were obtained as described before. After obtaining these monolayers to form LB films of quantum dots; these monolayers were transferred onto a solid substrate. This transfer named as deposition and this procedure described in section 1.2.3.

In all these LB deposition processes, first CdSe nanoparticle film was being formed at the air/water interface, and compressed to the desired surface pressure and particle density and then transferred onto a solid substrate by one of X and Z types dipping methods. For obtaining multilayers, the transfer of the film was repeated several times. The effects of deposition type and addition of surface active reagent as spacer were studied for the transfer of CdSe quantum dots LB films on to the substrate surface.

While working on the LB films of CdSe QDs deposition isotherms were obtained and shown in the next section. Moreover, transfer ratios of these dippings were studied. The effect of deposition type and adding spacer surface active reagent on the transfer ratio were studied for the preparation of CdSe quantum dots films and explained in section 3.6.2.

3.6.1. Deposition Isotherms

In the course of deposition studies, all cleaning procedures applied as mentioned before in section 2.3. The substrate was attached to the dipping arm and the zero line where the substrate starts to emerge or submerge for the substrate were determined and the solution was spread onto subphase. Before deposition studies; the target surface pressure that is determined from the monolayer isotherms and is entered to the system program. The target surface pressure is the pressure that monolayer

indicates solid like behaviour. After evaporation of solvent barriers starts to compression till the target surface pressure and at this surface pressure, the barriers try to keep constant pressure and movement of dipping arm starts depending on the deposition type. Over the course of this movement the transfer of the monolayer onto a solid substrate is done.

To obtain a quantum dot monolayer, deposition studies were done onto a glass substrate. Therefore, before deposition of the monolayer onto a glass substrate the hydrophobic treatment done onto the glass substrates as mentioned before (2.5 and 3.3).

For the deposition experiments we used the conditions as explained in section 3.4.1 and 3.4.2. According to these sections, 30 μL of CdSe quantum dot solution compressed at the rate of 10 mm/min was studied for deposition experiments. When surface pressure reached the target surface pressure the dipper of the LB system started to movement at a constant and set rate (5mm/min), and the transfer of monolayer on the substrate was done depending on the deposition type where mentioned before in section 1.2.3.

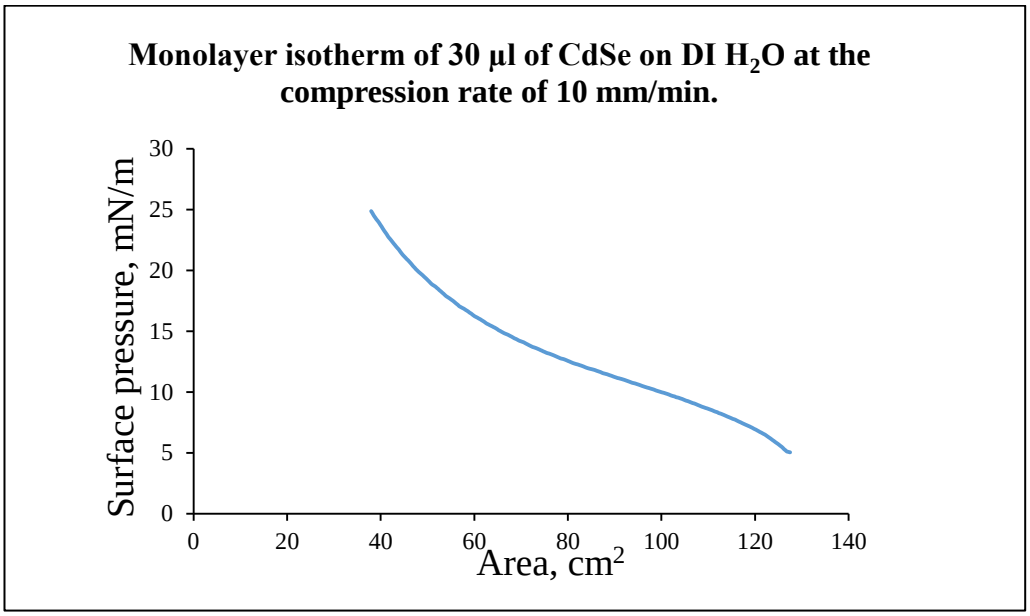

Figure 34 Monolayer isotherm of 30 µL of CdSe quantum dot solution at the compression rate of 10 mm/min that was obtained during the optimization studies

Figure 34 indicates the monolayer isotherm of 30 µL of CdSe quantum dot solution at the compression rate of 10 mm/min and Figure 35 indicates the same monolayer isotherm and deposition isotherms of two dipping isotherms at equal conditions but different days. In our studies surface pressure area isotherms established before and in the course of transfer process (dipping isotherm) were superimposing each other, Therefore, we were sure that the transfer process would be carried out at the predetermined optimum condition of the LB film.

At this point transfer ratio that was defined in section 2.6 is also significant and this issue studied on the next section.

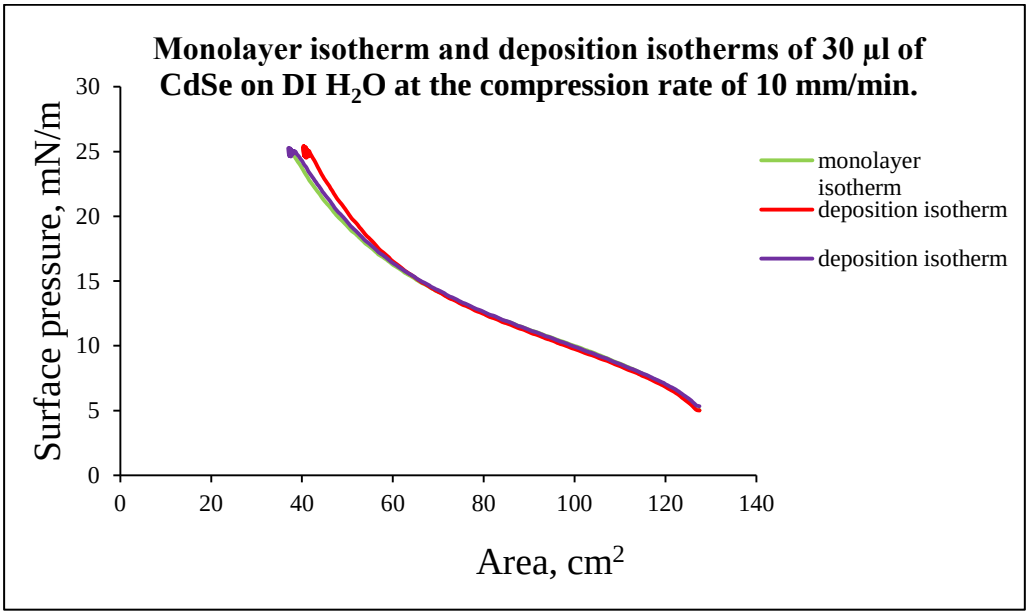

Figure 35 Monolayer isotherm and dipping isotherm of 30 µL of CdSe quantum dot solution at the compression rate of 10 mm/min that was obtained during the optimization and deposition studies

Beside this, the monolayer of SA – QD solution also studied as noticed on the section 3.4.2. According to the obtained data from this part, the deposition experiments of mixture of the SA and CdSe QD solution studied. Figure 36 indicates the monolayer and deposition isotherms of 20 µL of mixture of CdSe – SA solution.

Furthermore, Π-Area isotherms for the monolayer formation of the mixture of the SA and CdSe QD solution obtained independent of transfer process and during the transfer of the monolayer to the substrate were revealed the same the overlapping attitude, Figure 36.

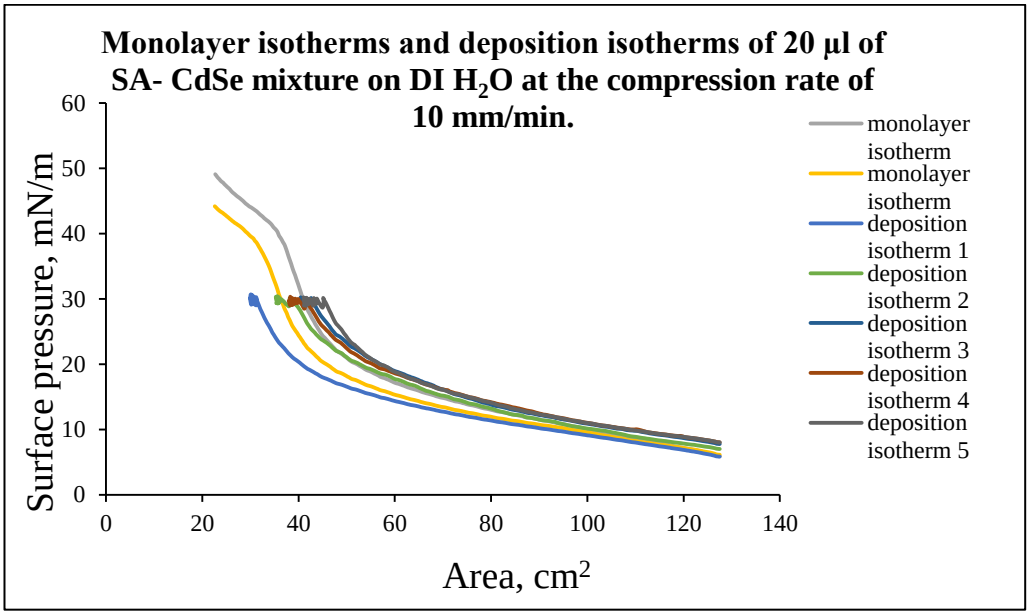

Figure 36 Monolayer and deposition isotherms of 20µL of SA and CdSe mixture at the compression rate of 10 mm/min

As it could be seen from Figure 37, the same result that can concluded for QD solution, could be finalized for deposition experiments of mixed SA – QD solution. Moreover, Figure 37 also indicates and supports the overlapping of the all dipping isotherms that were done. That is, the transfer process carried out at the predetermined optimum condition of the LB film. Transfer ratio studies were done also for the mixed solution of SA and CdSe QD and will be explained in the next section.

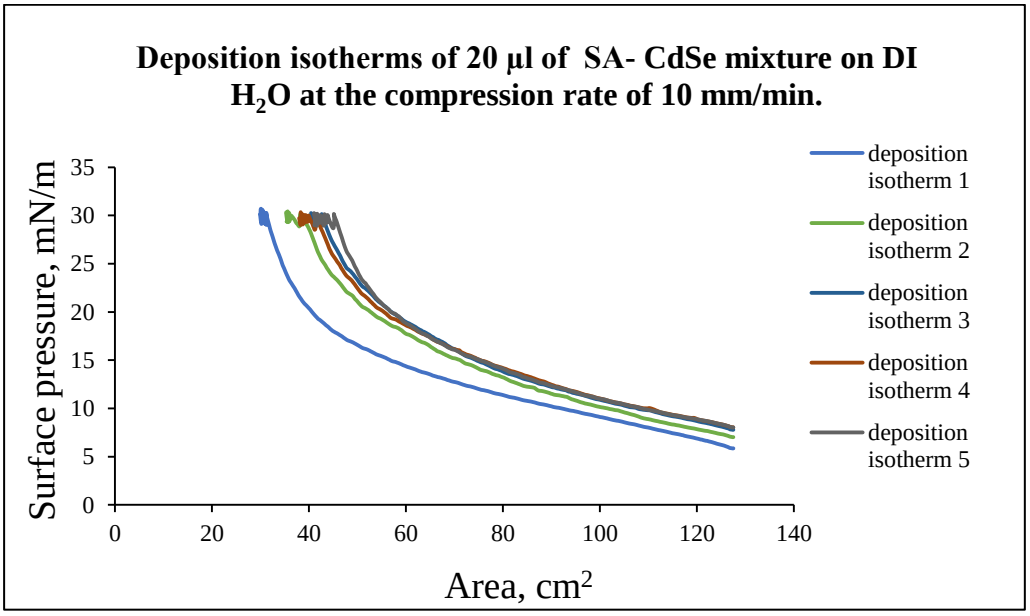

Figure 37 Deposition isotherms for 20 µL of SA and CdSe mixture at the compression rate of 10 mm/min

Furthermore, as a characterization method of LB film of CdSe QD one layer of CdSe QD solution deposited onto the TEM grid. The deposition was done with 20 µL of CdSe QD solution with compression rate 10 mm/min and at the target surface pressure 23 mN/m. The images and the result will be given oncoming section 3.7.2. When we look for the monolayer and deposition isotherm of transferring onto a TEM grid we determined the reproducibility of the formation of the monolayer on the air water interface as shown in Figure 38.

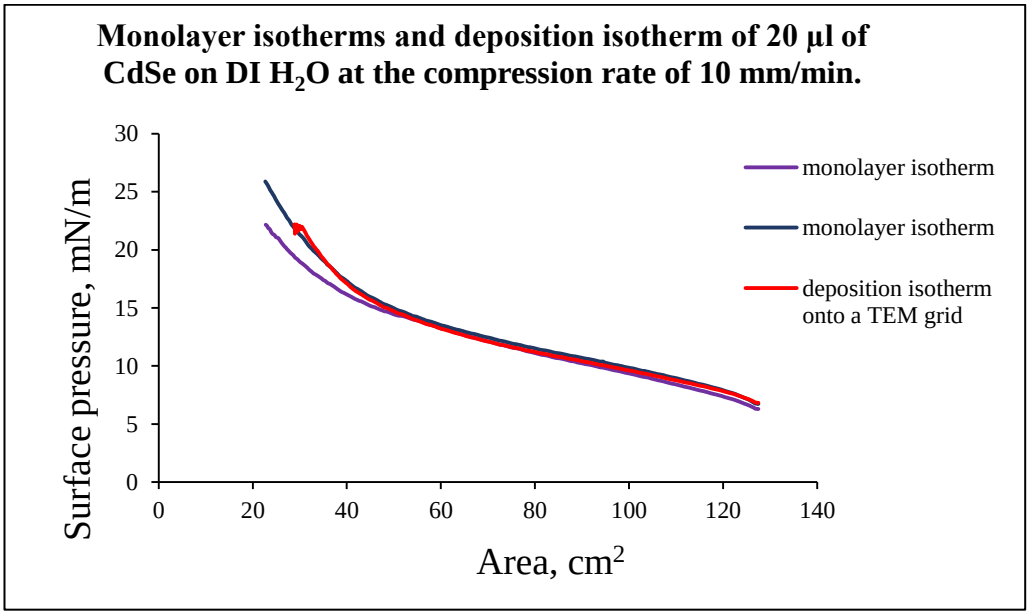

Figure 38 Monolayer and deposition isotherm onto a TEM grid of 20 µL of CdSe mixture at the compression rate of 10 mm/min

The transfer ratio and other characterization methods will be discussed oncoming section for all the deposition isotherms that was mentioned in this section.

For the monolayer and deposition experiments of quantum dots other optimization studies will be done as will be mentioned at the conclusion part.

3.6.2. Effect of Deposition Type on Transfer Ratio of CdSe Quantum Dot Monolayers

To observe the effect of deposition type on transfer ratio (decreasing area of monolayer on surface of subphase / monolayer capped area of support) of CdSe quantum dot monolayers X type (down-down-down) dipping and Z type (up-up-up) dipping were studied. For both deposition types, the same monolayer formation conditions were utilized. 20 µL of CdSe solution was dispersed in chloroform and compressed with a barrier rate of 10mm/min. First of all, hydrophobic glass plate was chosen as a substrate and the monolayer was deposited by dipping the substrate into the subphase at each transfer process (X type dipping). 19 multilayers of QDs

were deposited and transfer ratios were collected for each transition. Collected data are given at Table1.

Table 1 Transfer ratios obtained for each transfer through repeated X- type deposition of 19 layers

Number of Dipping	**Transfer Ratio**
Dipping 1	T.R. (↓):0.6
Dipping 2	T.R. (↓):0.4
Dipping 3	T.R. (↓):0.3
Dipping 4	T.R. (↓):0.5
Dipping 5	T.R. (↓):0.6
Dipping 6	T.R. (↓):0.5
Dipping 7	T.R. (↓):0.6
Dipping 8	T.R. (↓):0.5
Dipping 9	T.R. (↓):0.7
Dipping 10	T.R. (↓):0.5
Dipping 11	T.R. (↓):0.5
Dipping 12	T.R. (↓):0.4
Dipping 13	T.R. (↓):0.4
Dipping 14	T.R. (↓):0.2
Dipping 15	T.R. (↓):0.5
Dipping 16	T.R. (↓):0.6
Dipping 17	T.R. (↓):0.4
Dipping 18	T.R. (↓):0.6
Dipping 19	T.R. (↓):0.4

Secondly hydrophilic glass plate was used as a substrate, and deposition was done by lifting the substrate from the sub-phase to the air through the monolayer, Z- type deposition. The transfer ratios were collected for each transfer process and listed in Table 2. When transfer ratios for X-type and Z-type deposition were compared the transfer ratios obtained for Z- type deposition were more close to one, the ideal transfer ratio. Therefore, we preferred to continue with Z type deposition. Moreover, to observe the effect of the number of layers during repeated Z-type deposition on the transfer ratio, 6 consecutive layers were deposited and their transfer ratios were listed, Table 3.

Table 2 Transfer ratios obtained for each transfer through repeated Z- type deposition of 19 layers

Number of Dipping	**Transfer Ratio**
Dipping 1	T.R. (↑):0.2
Dipping 2	T.R. (↓):1.0
Dipping 3	T.R. (↑):0.7
Dipping 4	T.R. (↑):0.7
Dipping 5	T.R. (↑):1.0
Dipping 6	T.R. (↑):1.0
Dipping 7	T.R. (↑):1.6
Dipping 8	T.R. (↑):1.2
Dipping 9	T.R. (↑):0.6
Dipping 10	T.R. (↑):0.6
Dipping 11	T.R. (↑):0.6
Dipping 12	T.R. (↑):0.7
Dipping 13	T.R. (↑):0.4
Dipping 14	T.R. (↑):0.7
Dipping 15	T.R. (↑):0.4
Dipping 16	T.R. (↑):0.6
Dipping 17	T.R. (↑):0.9
Dipping 18	T.R. (↑):0.5
Dipping 19	T.R. (↑):0.6

Table 3 Transfer ratios obtained for each transfer through repeated Z- type deposition of 6 layers

Number of Dipping	**Transfer Ratio**
Dipping 1	T.R. (↑):1.0
Dipping 2	T.R. (↑):1.4
Dipping 3	T.R. (↑):1.5
Dipping 4	T.R. (↑):1.2
Dipping 5	T.R. (↑):0.7
Dipping 6	T.R. (↑):2.4

As it is seen from Table 2 and Table 3 as the number of layers increases transfer ratio decreases for the Z- type deposition.

According to the obtained transfer ratios; compared to 19 layers of CdSe quantum dots; 6 layers of CdSe quantum dots give better transfer ratios. These results also confirmed by the confocal microscopy images in the oncoming sections.

The transfer ratios obtained from the deposition of the mixture of the SA and quantum dot mixture are given in the Table 4. The transfer ratios due to the effect of SA increased more than expected that will be the result of the deposition of the formed monolayer during the compression. Addition of SA as a spacer; improves the monolayer ability and increase the transfer ratio of monolayer more than 1 onto a solid surface.

Table 4 Transfer ratios obtained for each transfer through repeated Z- type deposition of 5 layers of mixed solution of SA – CdSe QD

Number of Dipping	Transfer Ratio
Dipping 1	T.R. (↑):1.1
Dipping 2	T.R. (↑):1.7
Dipping 3	T.R. (↑):2.1
Dipping 4	T.R. (↑):1.9
Dipping 5	T.R. (↑):1.7

3.7. Characterization of Transferred Monolayer of CdSe QDs

The obtained LB films of CdSe quantum dots were tried to be characterized with confocal microscopy and transmission electron microscopy.

3.7.1. Confocal Microscopy

We were aware that resolution of the confocal microscopy was not sufficient to observe the nanometer size quantum dots on the glass substrate, however it might give us a quick information about the extent of the transfer of the QD particles on to the surface.

Confocal microscopy views of the 6-layer QD LB films on the substrate surface and the CdSe QD solution itself are shown in Figure 39. The fluorescence image for 5 layers of CdSe – SA mixture and 19 layers of CdSe QDs could not be observed under the light microscope.

According to Figure 39 b, there are several fluorescent rings on the surface resembling micron-sized micelle formation. In other words, it is understood that ODs are transferred to the surface, but no other information is available about the

arrangement of nanoparticles on the surface. For this reason, TEM measurements of LB films of QDs transferred to the substrate surface were performed.

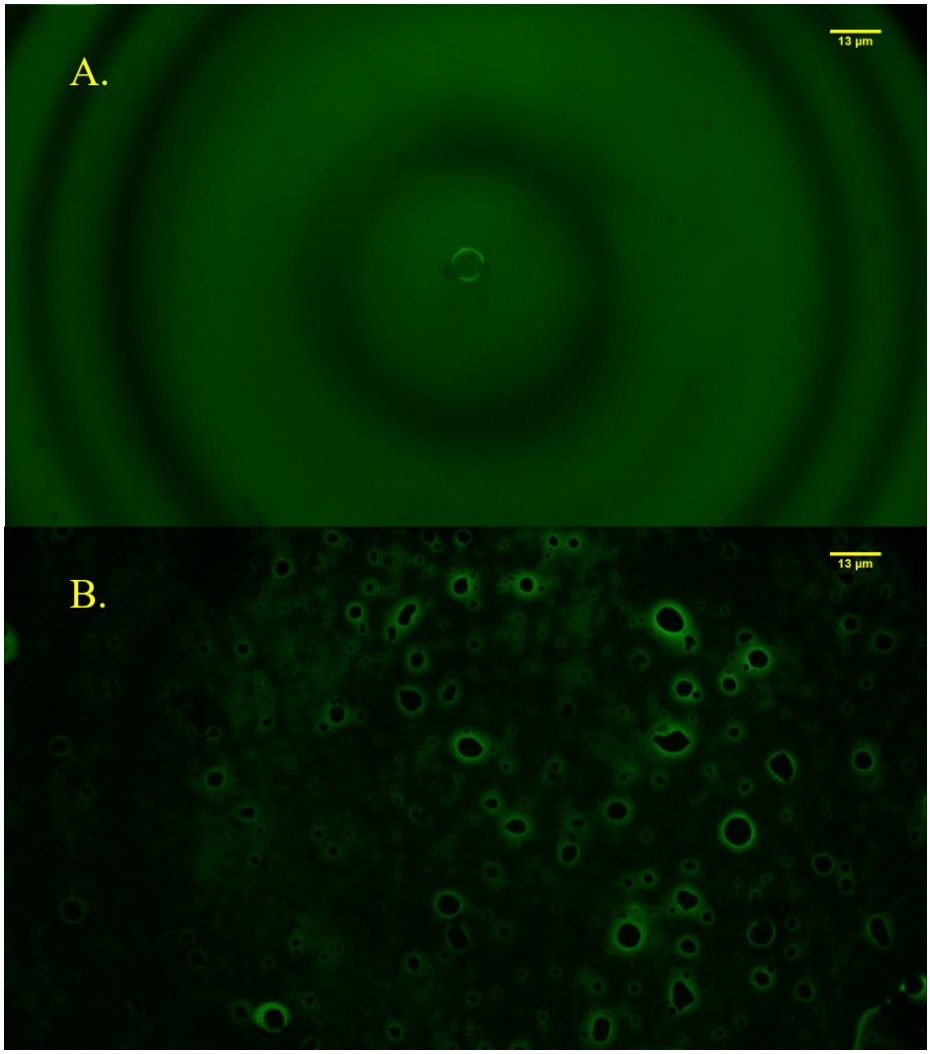

Figure 39 Image of a) CdSe solution and b) 6 layers of CdSe monolayers deposited onto a glass substrate

3.7.2. Transmission Electron Microscopy

To be sure about the deposition of the quantum dots monolayer obtained at the condition 20 μL of CdSe solution compressed with the barrier rate of 10 mm/min. The transfer was done at the surface pressure of 22 mN/m as given in the isotherms in the section 3.6.1.

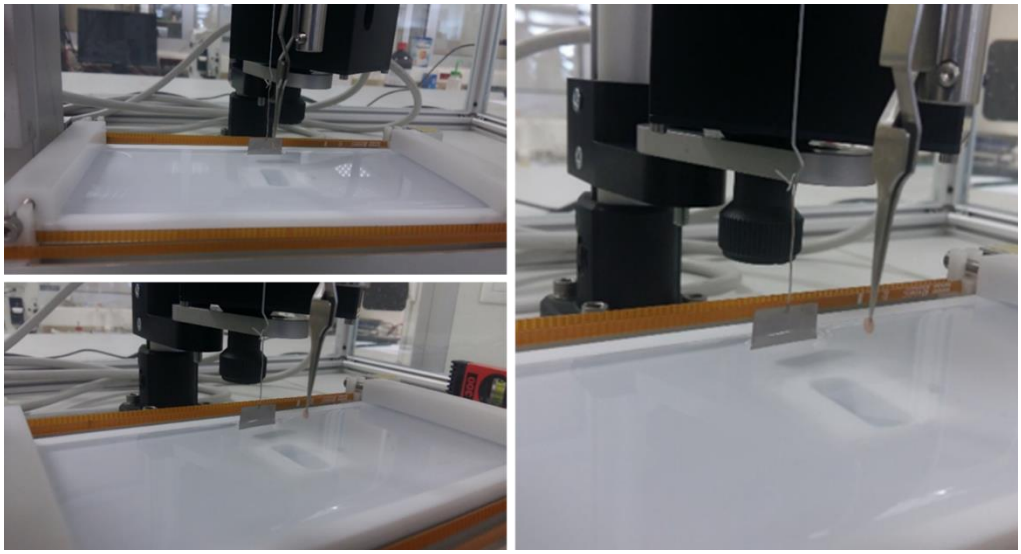

Figure 40 Images of dipping on a carbon coated cupper TEM grid

For this experiment with the help of tweezer copper coated TEM grid was placed to the dipper of the Langmuir Blodgett system as shown in the Figure 40.

The TEM images of the CdSe monolayer is deposited at surface pressure value 20 mN/m and as shown in the Figure 41 a and b at the 100 nm and 50 nm scale the CdSe monolayer was deposited onto a TEM grid successfully.

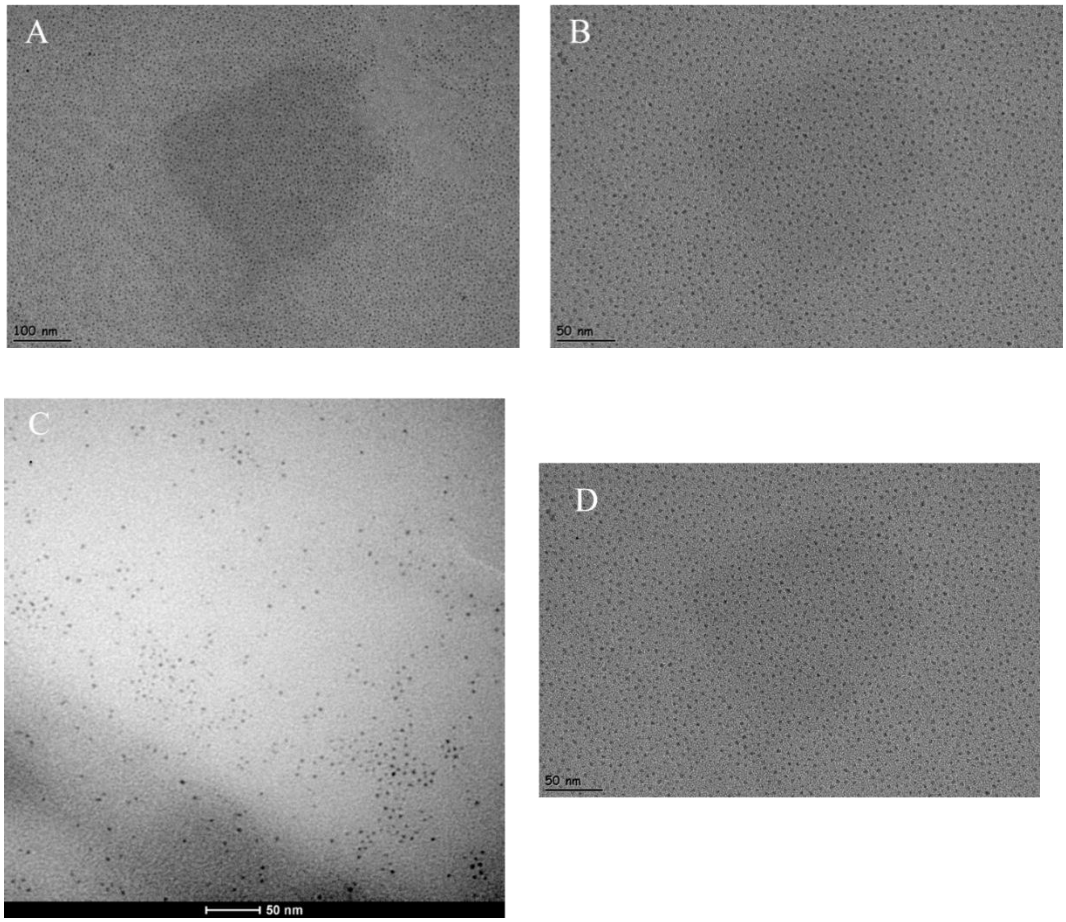

Figure 41 a) and b) TEM images of 1 layer of CdSe QDs Langmuir Blodgett film on carbon coated copper grid c) TEM image of CdSe QD solution obtained by dropping d) 1 layer of CdSe QDs Langmuir Blodgett film on carbon coated copper grid

Beside this, comparison of the same scale of TEM images of CdSe solution obtained by dropping a solution onto a TEM grid and monolayer of the CdSe quantum dots that transferred onto a TEM grid as shown in the Figure 41 c and d respectively. These images prove that the transferred monolayer was homogenous, arranged closely and orderly and free of microscopic voids over the coated area. Moreover, energy dispersive X-ray spectroscopy was applied to the same grid that monolayer transferred and the results also proves the presence of Cd and Se, and spectrum was given in Figure 42.

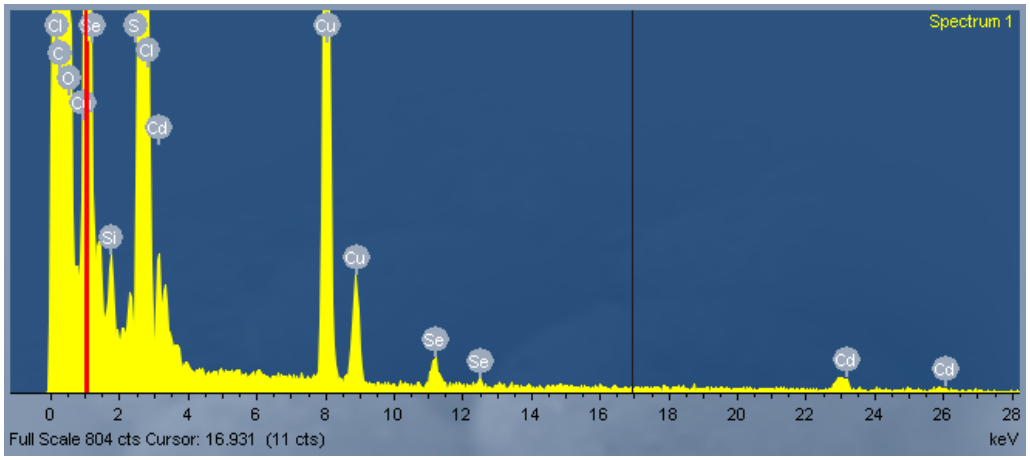

Figure 42 EDX spectrum of the CdSe quantum dot monolayer onto a TEM grid

.

CHAPTER 4

CONCLUSION

Thin films of molecules and nanostructures have a wide range of application due to their configurable properties by changing their tendency to arrangement. The technique of Langmuir and Langmuir Blodgett provides the controllable way of arrangement of the materials and nanostructures with the sensitivity of a molecular thickness.

Our goal was to homogeneously coat the various surfaces with LB technique so as not to leave spaces between the nanoparticles. We first decided to work on the difficulties we faced while preparing the thin films of the silver nanoparticles in the previous graduate study [55]. At the end of these studies, we decided to work with fluorescent nanoparticles, hoping that the success of the coating could be followed by a simple process like a hand-held UV lamp. Because of the wide application areas of thin films of CdSe QDs, the studies have been continued with these fluorescencing particles.

The monolayer formation of hexadecyltrimethylammonium bromide (CTAB) on deionized water and aqueous solution of poly(4-styrenesulfonate) (PSS) had studied previously in our laboratory and surface pressure – mean molecular area isotherms (π -MMA) were obtained. In this study firstly, the monolayer formation of CTAB at low concentration (0.07 mg/mL) was studied since thin films of silver nanoparticles was aimed to study with Langmuir Blodgett technique and at optimized conditions (50 μL of 0.07 mg/mL CTAB solution with the compression rate of 10 mm/min) the proper monolayer formation was obtained by using poly(4-styrenesulfonate) (0.1

mM, 1mM, 5mM and 10mM) as a gluing reagent. The difference between the isotherms of CTAB that were obtained on the water and aqueous solution of PSS subphase can be seen in Figure 43.

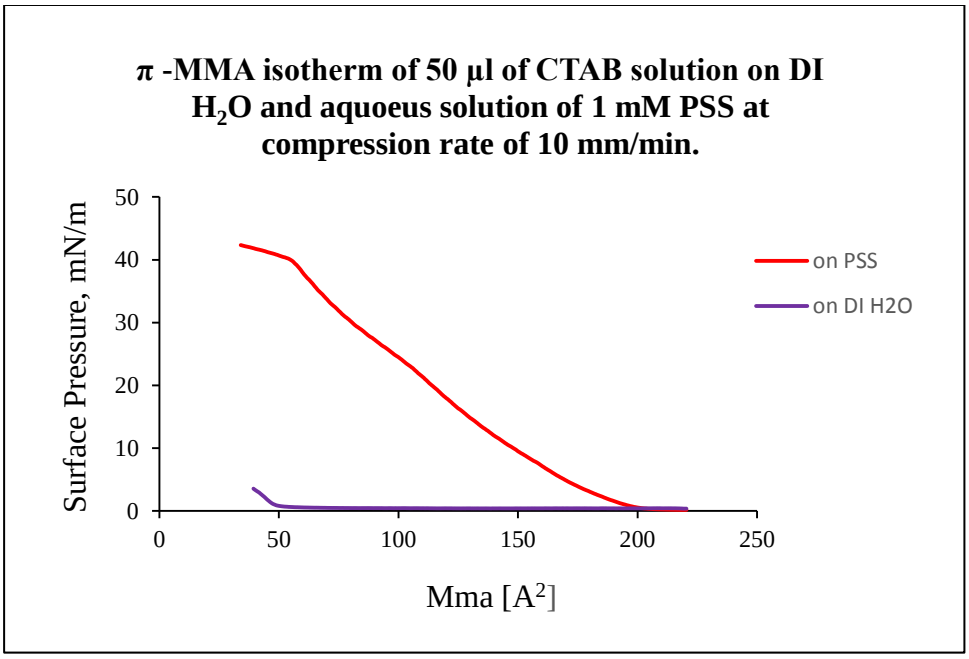

Figure 43 The monolayer isotherm of 50 µL of CTAB on DI H_2O and aqueous solution of 1mM PSS at compression rate of 10 mm/min

The monolayers of CTAB on the air water interphase formed successfully with gluing technique at 20°C.

Secondly, CdSe quantum dots synthesized with thermal decomposition method. For purification of QDs two method which were extracted with equal volumes of hexane and methanol and centrifuging with ethanol were done. The characterization of quantum dots was done with Fluorescence Spectrometer and Transmission Electron Microscopy (TEM). Though the former one was stated as a size dependent purification of the particles, the outcome of the TEM results were not as expected. Moreover, the results revealed that ethanol method was more effective for

purification. CdSe QDS were synthesized in narrow size distribution, 2-4 nm at the emission wavelength of 558 nm at the excitation wavelength of 400 nm.

The formation of monolayer of CdSe quantum dots were optimized by varying spread volume onto subphase and at optimized conditions (30 μL of QD solution with the compression rate of 10 mm/min) reproducible and stable monolayers were obtained on water subphase at 23°C.

Moreover, by mixing stearic acid (SA) solution with CdSe quantum dots solution effect of SA that was used as a spacer was studied. With the effect of SA, the collapse point of the π- A isotherm of the mixture was observed clearly.

After obtaining reproducible and stable formation of monolayers of CdSe quantum X type (down- down- down) and Z type (up- up- up) deposition methods was done on to the glass substrates and transfer ratios were collected. When the transfer ratios compared, Z type deposition provided better transfer ratios which were closer to 1. Moreover, collected transfer ratios showed that with increasing of the layers the transfer ratio decreases. Beside this the transfer of mixed SA- CdSe quantum dot monolayers was done and transfer ratios were compared with other experiments' transfer ratios and concluded as, with the effect of SA the ratio was increased.

The transferred monolayer onto glass substrates were characterized with confocal microscopy. In the image of the confocal microscopy fluorescent rings were seen in micron scale that resembled the transfer of CdSe quantum dots. Yet these images did not give any information about the arrangement of the particles, TEM grid was used as substrate and the monolayer transferred onto the grid. In Figure 44 and 45 the TEM images of CdSe QD onto a TEM grid in a scale of 100 nm and 50 nm for comparison was given.

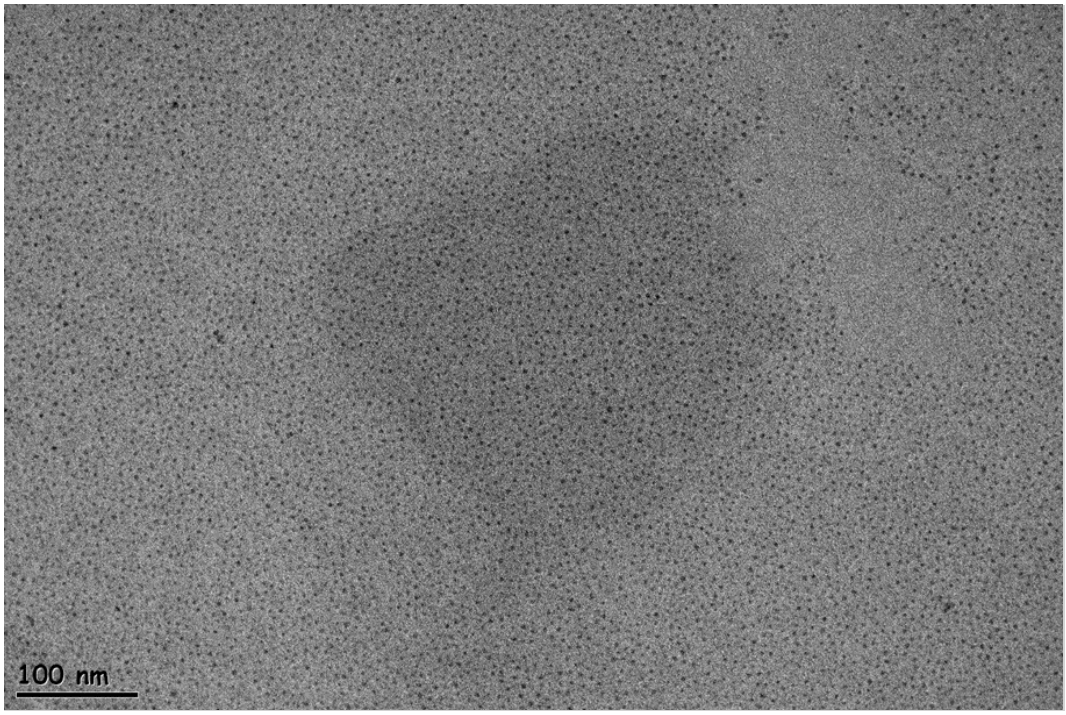

Figure 44 TEM image of 1 layer of CdSe QDs Langmuir Blodgett film on carbon coated copper grid in a scale of 100 nm

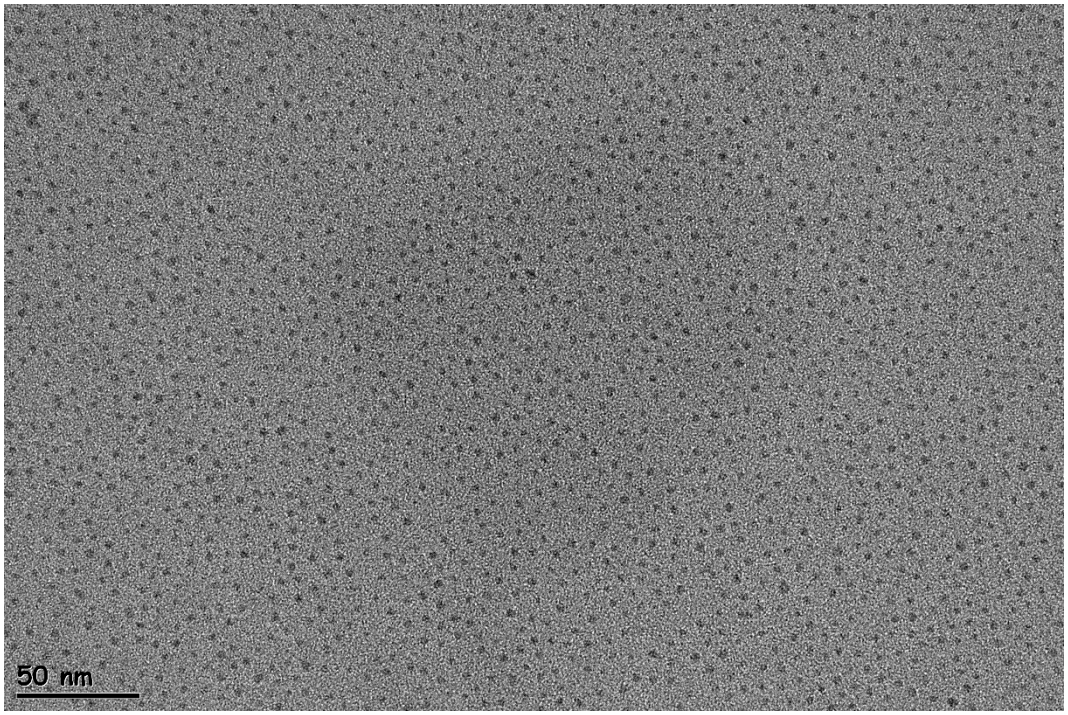

Figure 45 TEM image of 1 layer of CdSe QDs Langmuir Blodgett film on carbon coated copper grid in a scale of 50 nm

The images of the TEM demonstrate that the transferred monolayer was homogenous, arranged closely and orderly and free of microscopic voids over the coated area.

As a future work, studies are in progress and being aimed to define and complete the full scope of the monolayer and Langmuir Blodgett films of the CdSe quantum dots in terms of concentration, deposition optimization and thickness property.

REFERENCES

[1] F. Schreiber, "Structure and growth of self-assembling monolayers," *Prog. Surf. Sci.*, vol. 65, no. 5–8, pp. 151–256, 2000.

[2] A. Gole, N. R. Jana, S. T. Selvan, and J. Y. Ying, "Langmuir Blodgett Thin Films of Quantum Dots: Synthesis, Surface Modification, and Fluorescence Resonance Energy Transfer (FRET) Studies," *Langmuir*, vol. 24, no. 15, pp. 8181–8186, 2008.

[3] E. Gomar-Nadal, J. Puigmartı´-Luis, and D. B. Amabilino, "Assembly of functional molecular nanostructures on surfaces," *Chem. Soc. Rev.*, vol. 37, no. 3, pp. 490–504, 2008.

[4] R. K. Smith, P. A. Lewis, and P. S. Weiss, "Patterning self-assembled monolayers," *Prog. Surf. Sci.*, vol. 75, no. 1–2, pp. 1–68, 2004.

[5] D. R. Talham, "Conducting and Magnetic Langmuir - Blodgett Films," *Chem. Rev.*, vol. 104, no. 11, pp. 5479–5502, 2004.

[6] K. Ariga, Y. Yamauchi, T. Mori, and J. P. Hill, "25th Anniversary Article: What Can Be Done with the Langmuir-Blodgett Method? Recent Developments and its Critical Role in Materials Science," *Adv. Mater.*, vol. 25, no. 45, pp. 6477–6512, 2013.

[7] S. Ahmadi, N.Asim, M.A. Alghoul, F.Y. Hammadi, K. Saeedfar, N.A. Ludin, S.H. Zaidi, and K. Sopian, "The Role of Physical Techniques on the Preparation of Photoanodes for Dye Sensitized Solar Cells," *Int. J. Photoenergy*, vol. 2014, no. February, 2014.

[8] Y. Wang, A. S. Angelatos, and F. Caruso, “Template Synthesis of Nanostructured Materials via Layer-by-Layer Assembly,” *Chem. Mater.*, vol. 20, no. 3, pp. 848–858, 2008.

[9] Z. Tang, Y. Wang, P. Podsiadlo, and N. A. Kotov, “Biomedical Applications of Layer-by-Layer Assembly: From Biomimetics to Tissue Engineering,” *Adv. Mater.*, vol. 18, no. 24, pp. 3203–3224, 2006.

[10] G. G. Roberts, “An applied science perspective of Langmuir-Blodgett films,” *Adv. Phys.*, vol. 34, no. 4, pp. 475–512, 1985.

[11] G. L. Gaines, “On the history of Langmuir-Blodgett films,” *Thin Solid Films*, vol. 99, no. 1–3, pp. ix–xiii, 1983.

[12] R. F. De Oliveira, A. De Barros, and M. Ferreira, *Nanostructured films: Langmuir-Blodgett (LB) and Layer-by-Layer (LbL)Techniques*. Elsevier Inc., 2016.

[13] M. C. Petty, *Langmuir-Blodgett films An Introduction*. Cambridge University Press, 1996.

[14] A. Ulman, *An Introduction to ULTRATHIN ORGANIC FILMS From Langmuir-Blodgett to Self -Assembly*. academic press, 1991.

[15] A. R. Tao, J. Huang, and P. Yang, “Langmuir - Blodgettry of Nanocrystals and Nanowires,” *Acc. Chem. Res.*, vol. 41, no. 12, pp. 1662–1673, 2008.

[16] M. Ando, Y. Watanabe, T. Iyoda, K. Honda, and T. Shimidzu, “Syntheses of Conducting Polymer Langmuir-Blodgett Multilayers,” *Thin Solid Films*, vol. 179, pp. 225–231, 1989.

[17] K. M. G. Jianmin Xu, Xiaojun Ji and R. M. L. as-Asfura, ChengshanWang, “Langmuir and langmuir-Blodgett films of quantum dots,” *Colloids Surfaces A Physicochem. Eng. Asp.*, vol. 284, pp. 35–42, 2006.

[18] G. T. Barnes and I. T. Gentle, *Interfacial Science*, Second edi. Oxford University Press, 2011.

[19] V. Kaganer, H. Möhwald, and P. Dutta, “Structure and phase transitions in Langmuir monolayers,” *Rev. Mod. Phys.*, vol. 71, no. 3, pp. 779–819, 1999.

[20] T. Roch, B. Schulz, and A. Scho, “Evaluating polymeric biomaterial – environment interfaces by Langmuir monolayer techniques Review,” *J. R. Soc. Interface*, vol. 14, pp. 1–18, 2017.

[21] Z. Matharu, G. Sumana, S. K. Arya, S. P. Singh, V. Gupta, and B. D. Malhotra, “Polyaniline Langmuir-Blodgett film based cholesterol biosensor.,” *Langmuir*, vol. 23, no. 26, pp. 13188–13192, 2007.

[22] I. Çapan, R. Çapan, T. Tanrisever, and S. Can, “Poly(methyl methacrylate) monolayers at the air-water interface,” *Mater. Lett.*, vol. 59, no. 19–20, pp. 2468–2471, 2005.

[23] X. Yan, V. Janout, J. T. Hsu, and S. L. Regen, “The gluing of a Langmuir-Blodgett bilayer,” *J. Am. Chem. Soc.*, vol. 125, no. 27, pp. 8094–8095, 2003.

[24] M. Wang, V. Janout, and S. L. Regen, “Minimizing Defects in Polymer-Based Langmuir- Blodgett Monolayers and Bilayers Via Gluing,” *Langmuir*, vol. 28, pp. 1–4, 2012.

[25] D. K. Lee, Y. H. Kim, C. W. Kim, H. G. Cha, and Y. S. Kang, “Vast Magnetic Monolayer Film with Surfactant-Stabilized Fe3O4 Nanoparticles Using Langmuir-Blodgett Technique,” *J. Phys. Chem. B*, vol. 111, no. 31, pp. 9288–9293, 2007.

[26] C. Liu, Y. Shan, Y. Zhu, and K. Chen, “Magnetic monolayer film of oleic acid-stabilized Fe3O4 particles fabricated via Langmuir-Blodgett technique,” *Thin Solid Films*, vol. 518, no. 1, pp. 324–327, 2009.

[27] G. Zhavnerko and G. Marletta, “Developing Langmuir-Blodgett strategies towards practical devices,” *Mater. Sci. Eng. B Solid-State Mater. Adv. Technol.*, vol. 169, no. 1–3, pp. 43–48, 2010.

[28] K. Lambert, Y. Justo, J. S. Kamal, and Z. Hens, “Phase transitions in Quantum-Dot Langmuir films,” *Angew. Chemie - Int. Ed.*, vol. 50, no. 50, pp. 12058–12061, 2011.

[29] T. E. Goto, C.C. Lopes, H.B. Nader, A.C.A. Silva, N.O. Dantas, J.R. Siqueira, L. Caseli, “CdSe magic-sized quantum dots incorporated in biomembrane models at the air-water interface composed of components of tumorigenic and non-tumorigenic cells,” *Biochim. Biophys. Acta - Biomembr.*, vol. 1858, no. 7, pp. 1533–1540, 2016.

[30] H. Weller, “Colloidal Semiconductor Q- Particles: Chemistry in the Transition Region Between Solid State and Molecules,” *Angew. Chemie Int. Ed. English*, vol. 32, no. 1, pp. 41–53, 1993.

[31] D. Bera, L. Qian, T. K. Tseng, and P. H. Holloway, “Quantum Dots and Their Multimodal Applications: A review,” *Materials (Basel).*, vol. 3, no. 4, pp. 2260–2345, 2010.

[32] M. C. Beard, J. M. Luther, A. G. Midgett, O. E. Semonin, J. C. Johnson, and A. J. Nozik, “Semiconductor Quantum Dots and Quantum Dot Arrays and Applications of Multiple Exciton Generation to Third-Generation Photovoltaic Solar Cells,” *Chem. Rev.*, vol. 110, pp. 6873–6890, 2010.

[33] P. Malik, J. Singh, and R. Kakkar, “A review on CdSe quantum dots in sensing,” *Adv. Mater. Lett.*, vol. 5, no. 11, pp. 612–628, 2014.

[34] A. Smith and S. Nie, “Semiconductor Nanocrystals: Structure, Properties, and Band Gap Engineering,” *Acc. Chem. Res.*, vol. 43, no. 2, pp. 190–200, 2009.

[35] T. Jamieson, R. Bakhshi, D. Petrova, R. Pocock, M. Imani, and A. M. Seifalian, “Biological applications of quantum dots,” *Biomaterials*, vol. 28, no. 31, pp. 4717–4732, 2007.

[36] A. Kazemi and M. Zamiri, “Colloidal and Epitaxial Quantum Dot Infrared Photodetectors: Growth, Performance, and Comparison,” *Wiley Encycl. Electr. Electron. Eng.*, no. 104, pp. 1–26, 2014.

[37] Y. Shirasaki, G. J. Supran, M. G. Bawendi, and V. Bulović, “Emergence of colloidal quantum-dot light-emitting technologies,” *Nat. Photonics*, vol. 7, no. 12, pp. 13–23, 2013.

[38] D. V Talapin, I. Mekis, S. Go, A. Kornowski, O. Benson, and H. Weller, “CdSe / CdS / ZnS and CdSe / ZnSe / ZnS Core - Shell - Shell Nanocrystals,” *J. Phys. Chem. B*, vol. 108, pp. 18826–18831, 2004.

[39] A. M. Munro, J.A. Bardecker, M.S. Liu, Y. Cheng, Y. Niu, I. J. Plante, A. K.Y. Jen, D.S. Ginger, “Colloidal CdSe quantum dot electroluminescence: Ligands and light-emitting diodes,” *Microchim. Acta*, vol. 160, no. 3, pp. 345–350, 2008.

[40] I. Mekis, D. V. Talapin, A. Kornowski, M. Haase, and H. Weller, “One-Pot Synthesis of Highly Luminescent CdSe/CdS Core−Shell Nanocrystals via Organometallic and ‘Greener’ Chemical Approaches †,” *J. Phys. Chem. B*, vol. 107, no. 30, pp. 7454–7462, 2003.

[41] M. L. Landry, T. E. Morrell, T. K. Karagounis, C. H. Hsia, and C. Y. Wang, “Simple Syntheses of CdSe Quantum Dots,” *J. Chem. Educ.*, vol. 91, no. 2, pp. 274–279, 2014.

[42] Z. A. Peng and X. Peng, “Formation of high-quality CdTe, CdSe, and CdS nanocrystals using CdO as precursor,” *J. Am. Chem. Soc.*, vol. 123, no. 1, pp. 183–184, 2001.

[43] J. M. Haremza, M. A. Hahn, T. D. Krauss, S. Chen, and J. Calcines, “Attachment of Single CdSe Nanocrystals to Individual Single-Walled Carbon Nanotubes,” *Nano Lett.*, vol. 2, no. 11, pp. 2–4, 2002.

[44] L. H. Qu, Z. a Peng, and X. G. Peng, “Alternative routes toward high quality CdSe nanocrystals,” *Nano Lett.*, vol. 1, no. 6, pp. 333–337, 2001.

[45] J. J. Li, A. Wang, W. Guo, J.C. Keay, T. D. Mishima, M. B. Johnson, X. Peng, "Large-Scale Synthesis of Nearly Monodisperse CdSe / CdS Core / Shell Nanocrystals Using Air-Stable Reagents via Successive Ion Layer Adsorption and Reaction," *Thin Solid Films*, no. 4, pp. 933–937, 2003.

[46] W. W. Yu and X. Peng, "Formation of high-quality CdS and other II-VI semiconductor nanocrystals in noncoordinating solvents: Tunable reactivity of monomers," *Angew. Chemie - Int. Ed.*, vol. 41, no. 13, pp. 2368–2371, 2002.

[47] K. Lambert, R. K. Capek, M. I. Bodnarchuk, M.V. Kovalenko, D.V. Thourhout, W. Heiss, Z. Hens, "Langmuir-schaefer deposition of quantum dot multilayers," *Langmuir*, vol. 26, no. 11, pp. 7732–7736, 2010.

[48] M. J. Hampton, J. L. Templeton, and J. M. Desimone, "Direct patterning of CdSe Quantum Dots into sub-100 nm structures," *Langmuir*, vol. 26, no. 5, pp. 3012–3015, 2010.

[49] S. Das, B. Satpati, H. Chauhan, S. Deka, C. S. Gopinath, and T. Bala, "Preferential Growth of Au on CdSe quantum dots using Langmuir–Blodgett technique," *Rsc Adv.*, vol. 4, no. 110, pp. 64535–64541, 2014.

[50] M. D. Goodman, J. Xu, J. Wang, and Z. Lin, "Semiconductor conjugated Polymer - Quantum dot Nanocomposites at the Air/Water Interface and Their Photovoltaic Performance," *Chem. Mater.*, vol. 21, no. 5, pp. 934–938, 2009.

[51] N. F. Crawford and R. M. Leblanc, "CdSe and CdSe(ZnS) quantum dots in 2D: A Langmuir monolayer approach," *Coord. Chem. Rev.*, vol. 263–264, no. 1, pp. 13–24, 2014.

[52] M. Y. Zhou, R. Xie, Y. L. Yu, G. Chen, X.J. Ju, L. Yang, B. Liang, L.Y. Chu,"Effects of surface wettability and roughness of microchannel on flow behaviors of thermo-responsive microspheres therein during the phase transition," *J. Colloid Interface Sci.*, vol. 336, no. 1, pp. 162–170, 2009.

[53] K. J. Nordell, E. M. Boatman, and G. C. Lisensky, “A Safer, Easier, Faster Synthesis for CdSe Quantum Dot Nanocrystals,” *J. Chem. Educ.*, vol. 82, no. 11, p. 1697, 2005.

[54] W. W. Yu, L. Qu, W. Guo, and X. Peng, “Experimental Determination of the Extinction Coefficient of CdTe , CdSe , and CdS Nanocrystals Experimental Determination of the Extinction Coefficient of CdTe , CdSe , and CdS Nanocrystals,” *Chem. Mater.*, vol. 15, no. 14, pp. 2854–2860, 2003.

[55] N. N. UTKU, “STABILIZATION OF LANGMUIR AND LANGMUIR BLODGETT CETYLTRIMETHYLAMMONIUM BROMIDE MONOLAYERS BY GLUING WITH POLYSTYRENE SULFONATE,” Middle East Technical University, 2015.

[56] J. M. Corkill, J. F. Goodman, S. P. Harrold, and J. R. Tate, “Monolayers Formed by Mixtures of anionic and Cationic Surface-Active Agents,” *Trans. Faraday Soc.*, vol. 63, pp. 247–256, 1967.

[57] A. Asnacios, D. Langevin, and J.-F. Argillier, “Complexation of Cationic Surfactant and Anionic Polymer at the Air−Water Interface,” *Macromolecules*, vol. 29, no. 23, pp. 7412–7417, 1996.

[58] S. S. Gayathri and A. Patnaik, “Interfacial behaviour of brominated fullerene (C60Br24) and stearic acid mixed Langmuir films at air-water interface,” *Chem. Phys. Lett.*, vol. 433, no. 4–6, pp. 317–322, 2007.

[59] S. Biswas, S. A. Hussain, S. Deb, R. K. Nath, and D. Bhattacharjee, “Formation of complex films with water-soluble CTAB molecules,” *Spectrochim. Acta - Part A Mol. Biomol. Spectrosc.*, vol. 65, no. 3–4, pp. 628–632, 2006.

[60] S. Biswas, D. Bhattacharjee, R. K. Nath, and S. A. Hussain, “Formation of complex Langmuir and Langmuir-Blodgett films of water soluble rosebengal,” *J. Colloid Interface Sci.*, vol. 311, no. 2, pp. 361–367, 2007.

[61] O. S. Esan, Olubunmi, O. Medinat, A. C. Olumuyiwa, and O. Olarenwaju, “Effects of Temperature and Tetramethylammonium Bromide Salt on the Micellization of Cetyltrimethylammonium Bromide in Aqueous Medium: A Conductometric Studies,” *Int. J. Thermodyn.*, vol. 18, no. 4, pp. 246–252, 2015.

[62] B. Tah, P. Pal, M. Mahato, and G. B. Talapatra, “Aggregation Behavior of SDS / CTAB Catanionic Surfactant Mixture in Aqueous Solution and at the Air / Water Interface,” *J. Phys. Chem. B*, vol. 115, pp. 8493–8499, 2011.

[63] J. Li, V. Janout, and S. L. Regen, “Glued Langmuir-Blodgett Film: An Unexpected Dependency of Gluing on Polyelectrolyte Concentration,” *Langmuir*, vol. 20, no. 6, pp. 2048–2049, 2004.

[64] J. Li, V. Janout, and S. L. Regen, “Gluing Langmuir - Blodgett Monolayers onto Hydrocarbon Surfaces,” *J. Am. Chem. Soc.*, vol. 7, pp. 682–683, 2006.

[65] S. Sudheesh, J. Ahmad, and G. S. Singh, “Hysteresis of Isotherms of Mixed Monolayers of N-Octadecyl-N′-phenylthiourea and Stearic Acid at Air/Water Interface,” *ISRN Phys. Chem.*, vol. 2012, pp. 1–6, 2012.

[66] C. B. Murray, D. J. Norris, and M. G. Bawendi, “Synthesis and Characterization of Nearly Monodisperse CdE (E = S, Se, Te) Semiconductor Nanocrystallites,” *J. Am. Chem. Soc.*, vol. 115, no. 4, pp. 8706–8715, 1993.

[67] A. Sharma, C. M. Pandey, Z. Matharu, U. Soni, S. Sapra, G. Sumana, M. K. Pandey, T. Chatterjee, B. D. Malhotra “Nanopatterned cadmium selenide langmuir-blodgett platform for Leukemia Detection,” *Anal. Chem.*, vol. 84, no. 7, pp. 3082–3089, 2012.